

Article

Comparison of Potato and Asian Citrus Psyllid Adult and Nymph Transcriptomes Identified Vector Transcripts with Potential Involvement in Circulative, Propagative *Liberibacter* Transmission

Tonja W. Fisher ¹, Meenal Vyas ¹, Ruifeng He ², William Nelson ³, Joseph M. Cicero ¹, Mark Willer ³, Ryan Kim ⁴, Robin Kramer ⁴, Greg A. May ⁴, John A. Crow ⁴, Carol A. Soderlund ³, David R. Gang ² and Judith K. Brown ^{1,*}

¹ School of Plant Sciences, The University of Arizona, Tucson, AZ 85721, USA; E-Mails: twfisher@email.arizona.edu (T.W.F.); molupapa@gmail.com (M.V.); jmc6@ag.arizona.edu (J.M.C.)

² Institute of Biological Chemistry, Washington State University, Pullman, WA 99164, USA; E-Mails: rfhe@wsu.edu (R.H.); gangd@wsu.edu (D.R.G.)

³ BIO5, The University of Arizona, Tucson, AZ 85721, USA; E-Mails: will@agcol.arizona.edu (W.N.); mark@agcol.arizona.edu (M.W.); cari@agcol.arizona.edu (C.A.S.)

⁴ National Center for Genome Resources, 2935 Rodeo Park Drive East, Santa Fe, NM 87505, USA; E-Mails: rwkim@ucdavis.edu (R.K.); robin.kramer@nih.gov (R.K.); gregory.may@pioneer.com (G.A.M.); john.crow@pioneer.com (J.A.C.)

* Author to whom correspondence should be addressed; E-Mail: jkbrown@email.arizona.edu; Tel.: 520-621-1402.

External Editor: Lawrence S. Young

Received: 19 September 2014; in revised form: 18 October 2014 / Accepted: 20 October 2014 / Published: 3 November 2014

Abstract: The potato psyllid (PoP) *Bactericera cockerelli* (Sulc) and Asian citrus psyllid (ACP) *Diaphorina citri* Kuwayama are the insect vectors of the fastidious plant pathogen, *Candidatus* *Liberibacter solanacearum* (CLso) and *Ca. L. asiaticus* (CLas), respectively. CLso causes Zebra chip disease of potato and vein-greening in solanaceous species, whereas, CLas causes citrus greening disease. The reliance on insecticides for vector management to reduce pathogen transmission has increased interest in alternative approaches, including RNA interference to abate expression of genes essential for psyllid-mediated *Ca. Liberibacter* transmission. To identify genes with significantly altered

expression at different life stages and conditions of CLso/CLas infection, cDNA libraries were constructed for CLso-infected and -uninfected PoP adults and nymphal instars. Illumina sequencing produced 199,081,451 reads that were assembled into 82,224 unique transcripts. PoP and the analogous transcripts from ACP adult and nymphs reported elsewhere were annotated, organized into functional gene groups using the Gene Ontology classification system, and analyzed for differential *in silico* expression. Expression profiles revealed vector life stage differences and differential gene expression associated with *Liberibacter* infection of the psyllid host, including invasion, immune system modulation, nutrition, and development.

Keywords: circulative-propagative transmission; fastidious plant bacteria; psyllid vector; transcriptome

1. Introduction

The potato/tomato psyllid (PoP), *Bactericera cockerelli* (Sulc) (Triozidae) is a hemipteran insect that colonizes mainly plant species in Convolvulaceae and Solanaceae. PoP transmits a recently discovered, fastidious bacterium that has been associated with the emergence of the plant diseases, zebra chip of potato (affecting leaves and tubers) and vein greening of tomato (affecting leaves and fruit) and other solanaceous species [1–3]. The causal agent is the phloem-limited bacterium, *Candidatus Liberibacter solanacearum* (CLso), also known as *Ca. L. psyllaourous* [4] that is transmitted by *B. cockerelli* [5]. Until recently, the potato psyllid was known only for its association with “psyllid yellows” disease of tomato, pepper, and potato plants, syndromes attributed to psyllid feeding alone and to a salivary toxin [6]. These observations strongly suggest that CLso emergence and PoP transmission of it is a recent phenomenon. In contrast, the Asian citrus psyllid (ACP), *Diaphorina citri* is well known as the vector of *Ca. L. americanus*, *asiaticus*, and *africanus*, also fastidious bacteria and the causal agents of citrus greening disease, or Huanglongbing (HLB) [7,8]. HLB has reached a crisis-level in the citrus industry worldwide [9].

The genus *Ca. Liberibacter* contains obligate, phloem-limited gram-negative bacteria classified in the α -Proteobacteria [10]. Both CLas and CLso multiply in both the plant and their psyllid host, and therefore utilize a circulative-propagative mode of transmission [11–15]. Evidence that CLas is detectable in ACP eggs by polymerase chain reaction (PCR) suggests a low level of transovarial transmission [4,16], however, additional evidence is needed for a direct role in the life cycle to confirm this observation. Also, transmission from ACP males to females has been reported based on qPCR detection in eggs that were dissected from uninfected females following mating with CLas-infected males [17]. The low frequency of CLas detection in ACP eggs and sexually, at 2%–6%, suggests that vertical transmission may be an important as a survival mechanism when a suitable CLas plant host is not available. Transmission electron microscopy (TEM) studies have revealed lesion-like pores on the external surfaces of CLso-infected PoP guts [18] that when taken together with reduced fecundity and nymphal survival for CLso-infected PoP [19,20], suggests CLso and perhaps other *Ca. Liberibacter* have evolved a parasitic relationship with their psyllid vector.

ACP and PoP harbor endosymbiotic bacteria, including the primary and secondary endosymbionts, *Carsonella ruddii* [21,22] and *Arsenophonus*, respectively, both α -Proteobacteria. In addition, *Wolbachia* sp., a parasitic bacterium most well known in arthropods for perturbing host reproduction [23], was detected in all nymphal and adult PoP life stages [22], and infecting 76.2% of ACP adults [24]. Psyllid defense responses, particularly those that counter invasion and nutritional deprivation [25], may exhibit species-specific host-parasite relationships, some which may depend on the duration of parasite-host exposure, and different interactions they have evolved with their endosymbionts [26]. Certain ACP endosymbionts require nitrogenous waste recycling and partitioning of other resources associated with ecological adaptations [27–29], a relationship that is mutually beneficial to them and their psyllid host [28–30]. In contrast, CLAs and CLso, which propagate and circulate in their psyllid host, may perturb the host innate immunity and other stress responses, while also exploiting host nutritional stores required for colonization, multiplication, circulation, acquisition, and transmission to the plant host.

Transmission efficiency of CLAs and CLso by ACP and PoP, respectively, appears to be dependent on the life stage of the vector during ingestion, and possibly also during the acquisition phase [11,16,31]. Transmission of CLAs by ACP adults has been shown to be most efficient when the bacterium is ingested during the nymphal stages, compared to adults [11,16]. This observation is supported by evidence that 40% of adult ACP given a 5-wk acquisition access period (AAP) on CLAs-infected plants were positive for CLAs ingestion, and yet when given an inoculation access period (IAP) to susceptible citrus seedlings, were unable to transmit the bacterium [16]. In contrast, 60% of ACP adults that ingested CLAs when reared from the egg through the adult stage on CLAs-infected plants transmitted the bacterium 73% of the time, when provided a 30-d IAP. This supports the observation that CLAs multiplication in the nymphal stages is essential for efficient adult-mediated transmission [11] but it does not rule out the possibility that the primary barrier to adult transmission is an insufficient titer of CLAs owing to ingested during adult instead of nymphal stages, and not an anatomical one.

In contrast, differences in CLso transmission frequency as a result of PoP life stage indicate that adult transmission between potato plants is 30% higher when psyllids are reared from egg to adult stage on CLso-infected plants, in comparison to nymphs when similarly reared on CLso-infected plants, despite each having a 7 d-IAP [31]. In another study, the 1st and 2nd PoP instars were found to have a lower CLso titer than the “older” 4th–5th nymphal stages or adults, observations that were supported by two respectively distinctive transcript profiles [32].

Similarly, taking into account clues from plant host responses to PoP feeding, gene expression studies in tomato plants colonized by CLso-infected PoP adults or nymphs showed that host gene expression was greatly affected by the particular life stage of CLso-infected psyllids, in that colonization by CLso-infected nymphs, compared to CLso-infected adults, resulted in the production of more differentially expressed plant transcripts [33]. Lastly, plant defense pathways known to be regulated by jasmonic acid and salicylic acid were suppressed in tomato plants exposed to the “older” nymphs and adults compared to 1st and 2nd nymphal instars.

Management of *Liberibacter*-incited diseases currently relies on insecticides to reduce the psyllid vector population and thereby the frequency of *Ca. Liberibacter* transmission [34,35]. The transmission cycle of *Ca. Liberibacter* in the psyllid is poorly studied. Only recently have studies suggested that *Ca.*

Liberibacter multiplies both in the plant and psyllid vector [12–16]. Understanding of the CLso and CLas circulative, propagative transmission pathway at the molecular, cellular, and functional genomics levels is of interest to enable the discovery of psyllid-Liberibacter interactions that can be targeted using RNA interference (RNAi) technology [36,37] or protein overexpression [38] to abate interactions essential for Liberibacter invasion, propagation, and transmission by the psyllid host.

The objective of this study is to determine gene expression profiles and use them to infer (predict) the basis for biological inference, based on *in silico* annotation of the differentially expressed genes of PoP and ACP adults and nymphs, reared from the egg to adult stages on CLas- and CLso-infected plants. A particular focus is the identification of differentially expressed psyllid genes predicted to be essential for direct or indirect interactions with Liberibacter effectors required for CLso and CLas to establish a circulative, propagative relationship with their PoP and ACP vector, respectively.

The transcript libraries produced for PoP psyllid adults and nymphs known to be infected with, or free of, CLso were sequenced using Next Generation Sequencing (NGS) Illumina technology and assembled into 82,224 *B. cockerelli* transcripts. Transcript comparisons were carried out using the Transcriptome Computation Workbench [39] and OrthoMCL software with an option for clustering. Using this approach it was possible to select a suite of differentially expressed contigs with a high degree of confidence from among the PoP and ACP (45,976) Illumina transcripts [40]. All databases have been made available with the TCW Java software, which can be queried at the website using the URL <http://www.sohomoptera.org/ACPPoP>.

A large number of up or down regulated psyllid genes (contigs) were identified and functionally annotated *in silico* using all available invertebrate (including insect), bacterial, viral databases. Among these a number of contigs of interest were mined, and found to have potential involvement in *Ca. Liberibacter* infection, adhesion, multiplication, and biofilm formation, as well as in host-parasite nutrient partitioning in the gut, circulation of Liberibacter in the hemolymph, and in entry into and acquisition by the salivary glands. The gut, hemolymph, and salivary glands have been implicated in CLas and CLso infection and propagation (entry, adhesion, multiplication), circulation, and association with the salivary gland region based on TEM and light microscopic localization studies [12–16,18,41] and validation by quantitative PCR detection [13–16,42]. Also, because the structure of the alimentary canal of ACP and PoP adults were found to be highly similar, it is considered likely that the circulative, propagative route of *Ca. Liberibacter* in anatomical context would be similar for both vectors, ACP and PoP [43]. In part, the functional genomics results supported this general hypothesis, while at the same time, despite conserved anatomical homologies, ACP and PoP adults and nymphs were found to respond differently to infection by their particular *Ca. Liberibacter* parasite. This was particularly striking for a set of genes with predicted functions in adhesion and immunity that were found to be differentially expressed in ACP nymphs but not particularly activated in the adults. In contrast, CLso invasion of PoP resulted in greatly perturbed gene expression in adults compared to nymphs. Thus, the parasitic strategies of these *Ca. Liberibacter* species appear to be uniquely related to the particular Liberibacter-psyllid complex. These differences may be found to be indicative of additional stage-specific characteristics, including the distinct transmission phenotypes observed for ACP and PoP adults and nymphs, respectively.

2. Results and Discussion

2.1. Assembly and Annotation of Potato Psyllid Transcriptomes

Four Illumina paired-end libraries were constructed for four treatments: whole bodies of the uninfected potato psyllid adults (Wb); whole bodies of *Liberibacter*-infected potato psyllid adults (WbL), uninfected potato psyllid nymphs (Ny), and *Liberibacter*-infected potato psyllid nymphs (NyL). Each library was sequenced in a single lane in an Illumina flow-cell using the Genome Analyzer Iix platform (Illumina, San Diego, CA, USA) to generate 2×54 bp independent reads from either end of a 250 ± 25 bp insert library fragment, resulting in a total of 199,081,451 clean reads, including 46,681,564 reads from library Wb, 53,240,863 reads from library WbL, 43,322,502 reads from library Ny and 55,836,522 reads from library NyL (Supplementary Table S1). High-quality reads were assembled to produce 82,224 contigs, 53.4 Mb in size, with an average length of 651 bp and distribution ranging from 100 to 27,405 bp in length: at 64% > 200 bp, 31% > 500 bp and 17% >1000 bp (Figure 1A). The average GC content of contigs was 40.6% and ranged from 12.1% to 82.4%. Contigs averaged 2421 sequencing reads (total expression level) and 17 reads per kilobase per million reads (RPKM). Within the TCW, the edgeR statistical software [44] was executed and the results entered into a database for query. More than 20% of contigs were significantly, differentially expressed, using a *p*-value cutoff of 0.05. The majority of differences were between the NyL \times WbL and Ny \times Wb comparisons, having the greatest number of differentially, expressed contigs (Figure 1B).

Of the 82,224 PoP contigs, 16,762 (20%) were annotated *in silico* to produce 28.9 Mb of sequence data, with N50 [45] and average lengths of 1390 bp and 1756 bp, respectively. The annotated contigs ranged in size from 100 to 27,405 bp with 91% > 200 bp, 76% > 500 bp, and 60% > 1000 bp (Figure 1A). Expression of the total annotated contigs comprised of 8212 sequencing reads (total) and 33 RPKM (Supplementary Table S1).

Most annotated PoP and ACP contigs [40] shared their greatest homology with sequences in the invertebrate UniProt database [46,47]. The potato psyllid (PoP) transcriptome contained more reads, at 199.1 million compared to the ACP transcriptome (129.6 million) and had a larger assembly size (53.4 Mb vs. 50.7 Mb) and more transcripts (82,224 vs. 45,976). But, PoP contigs were overall shorter on average, at 651 bp compared to ACP at 1106 bp. The lower percent of annotated PoP contigs at 20%, compared to 30% for ACP could suggest true intraspecific genomic differences between the two psyllids species, or it could possibly be due to differences in the average length of the contigs, even though the RNA quality was comparable for both.

Based on species-level homology, ACP and PoP showed a similar trend (Figure 2) in percentage of contigs with matches to pea aphid (*Acyrtosiphon pisum*) genes, at 15% for PoP and 17% for ACP. The next closest shared homology with other insects was in descending order for PoP and ACP, respectively, the red flour beetle (*Tribolium castaneum*) at 10% and 11%, body louse (*Pediculus humanus corporis*) at 9% and 11%, and fruit fly (*Drosophila melanogaster*) at 6% and 5%.

Figure 1. (A) The distribution of the lengths of potato psyllid contigs. The 199,081,451 high-quality Illumina reads determined from *Ca. Liberibacter solanacearum*-infected and uninfected adult or nymphal stage of the potato psyllid were assembled to yield 81,682 contigs, with a total size of 53.4 Mb, and average length of 654 base pairs (bp) that ranged in length from 100 to 27,405 bp; (B) The percentage of differentially expressed potato psyllid contigs among the different libraries and treatments at different *p*-values, based on EdgeR statistical analysis.

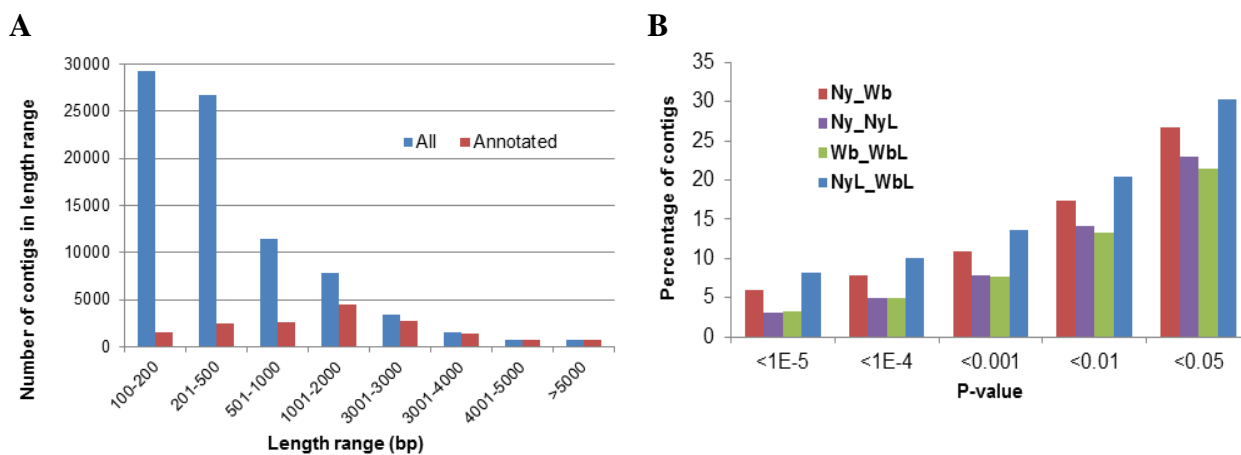
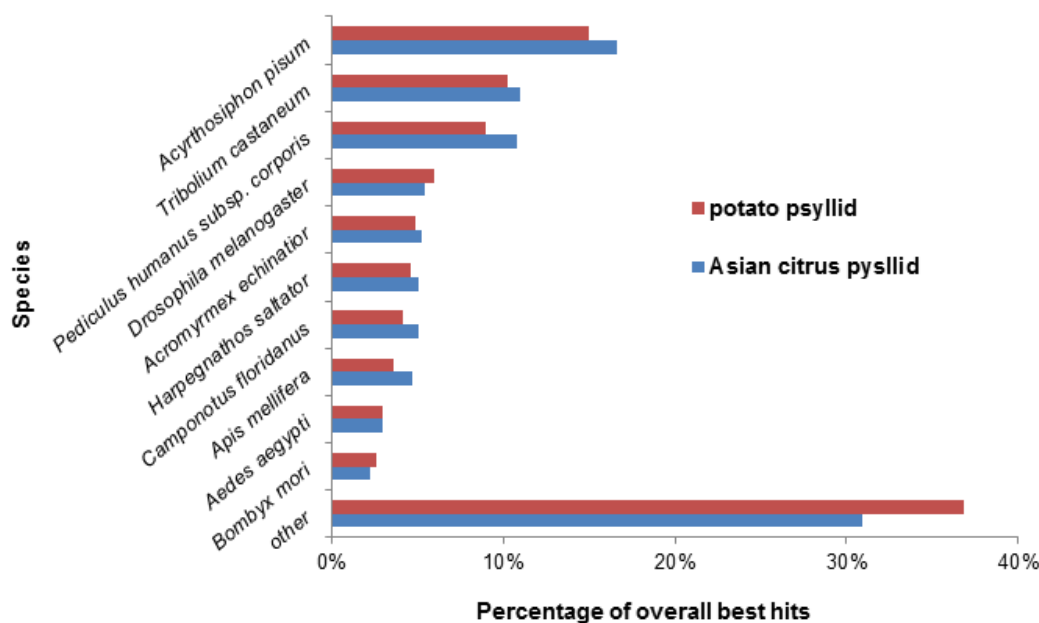


Figure 2. Species distribution of annotated contigs of adults and nymphs of the potato psyllid and Asian citrus psyllid. Data represent species of the first best hit obtained when contigs were blasted against the Swiss-Prot and Translated European Molecular Biology Laboratory (TrEMBL) protein databases for bacteria, invertebrates, and viruses. The majority of the annotated contigs matched to invertebrate-like proteins. The potato and Asian citrus psyllids shared similar overall homologies with the annotated contigs available for other insect species. The highest percentage of matches was to the pea aphid (*Acyrtosiphon pisum*).

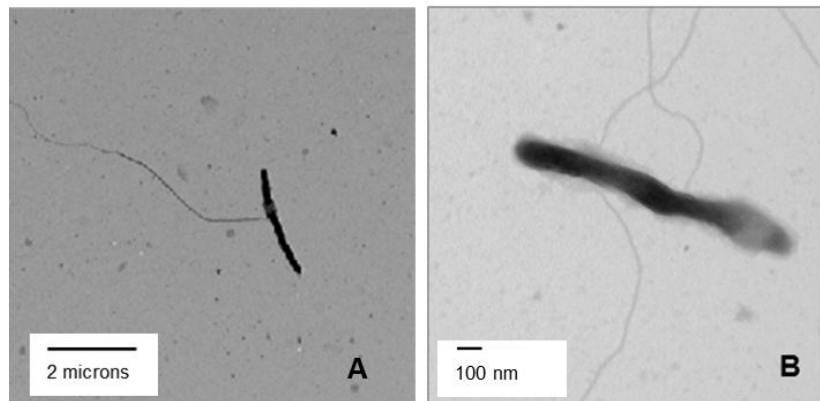


Most of the potato psyllid contigs (49%) annotated by bacterial databases available in SwissProt or TrEMBL were found to represent *Wolbachia* (GI:58535449) transcripts, and the remainder, approximately 18%, were mapped to the CLso genome (GI:313495152) sequence. The bacterial transcripts are thought to have been co-isolated with PoP transcripts. This is consistent with CLso presence in PoP and with previous knowledge of PoP infection by *Wolbachia* [22]. Manipulation of this naturally occurring *Wolbachia* sp. could possibly provide a vehicle for transgene delivery to the psyllid host [48].

Nachappa *et al.* [22] associated the bacterial species *Ca. Carsonella ruddii*, *Wolbachia*, CLso, *Acinetobacter*, and *Methylibium* with CLso-infected and -uninfected potato psyllids. The (contaminating) bacterial contigs reflected in our dataset shared no similarity to *Acinetobacter* or *Methylibium* transcripts. However 2% were from the primary endosymbiont, *Ca. C. ruddii* [49]. In addition, the bacterial contigs matching CLso genes were found only in the CLso-infected PoP libraries and comprised 84% of the total bacterial transcriptome. Even though these bacterial transcripts were unintentionally co-isolated with psyllid transcripts, it is apparent that not all five bacteria harbored by PoP were represented in the final dataset. This is possible due to their differential localization in psyllid tissues and organs, some of which were not specifically enriched for in library construction, and/or perhaps to differences in transcript copy number.

Among the CLso contigs, the most interesting with respect to adhesion, invasion-virulence, and potential motility were the pilus- and flagellar-related genes, and further of interest was that they were expressed at levels sufficient to detect them. The genome sequences of CLso and CLas (GI: 342316098) are known to encode these genes [8,50], and the CLas flagellin gene has been shown to be expressed as a functional protein [51]. Here, we used TEM to visualize long, strand-like appendages, sometimes alone or in multiples, emanating from the sides of some CLso cells on negative-stained grids (Figure 3). The appendages averaged 4 μm in length and were strikingly similar in appearance to the flagella and/or pilus-like structures of *Ralstonia solanacearum* reported by Wairuri *et al.* [52]. Also, the expression has been validated for several flagellar and pilus-like bacterial transcripts that were assembled with PoP transcript libraries by reverse transcriptase PCR (RT-PCR) [41; JX629450 and JX629449]. These transcripts were expressed only in CLso-infected psyllids suggesting they are encoded in the *Ca. Liberibacter* genome. Interference with expression of flagellar- or pilus-like genes could *Liberibacter* motility and/or adhesion of CLso/CLas within the psyllid, and possibly, in the host plant as well.

Figure 3. Negative-stained transmission electron micrograph from *Candidatus Liberibacter solanacearum* (CLso)-infected potato psyllid (PoP) hemolymph showing putative pilus- or flagella-like appendages of CLso.



Seven additional psyllid contigs were annotated as a ferroxidase-like enzyme (E-values, of E-12 to E-78), feasibly functioning in iron metabolism. Up-regulation of this psyllid enzyme in response to CLso infection could indicate induction by a CLso virulence factor(s) [53]. The CLso genome contains no annotated ferroxidase-coding regions, indicating the psyllid host may provide the CLso requirements for this enzymatic function. Down-regulation of a psyllid gene such as the latter seems strikingly essential for iron-metabolism in *Liberibacter*, and so could reduce iron availability that would result in starvation of the host, inadvertently undermining CLas/CLso multiplication. Thus, the effect of down-regulating the enzyme also could be detrimental to psyllid host survivability.

A large number of contigs (6.3%) were annotated using the viral sequence database in SwissProt and TrEMBL that shared homology with phage- and non-phage-like proteins. Several non-phage matches were found to the *Nuclear polyhedrosis virus* (NPV) and to densovirus-like sequences. Several NPV-related genes shared homology with cathepsin and an ecdysteroid UDP-glucosyltransferase, both genes whose expression could be detrimental to psyllid tissue integrity and potentially support CLas infection [54,55].

2.2. Effects of Potato Psyllid Adult and Nymph Life Stages, and *Liberibacter* Infection on Gene Expression

Psyllids are hemimetabolous insects and have morphologically distinct juvenile and adult stages. Both vector age and lifespan have been shown to be determinants of transmission efficiency [56], and *Ca. Liberibacter* has been reported to reduce the lifespan of PoP [19,20]. Laboratory and field studies have shown that PoP adults compared to nymphs, and ACP nymphs rather than adults, are the chief life stages involved in *Ca. Liberibacter* transmission [11,15–16,31]. PoP adults reared on CLso-infected plants were shown to transmit CLso with 100% efficiency, given a one-day inoculation access period (IAP) [31], compared to ACP adults reared on CLas-infected citrus plants, at 6.3% [16]. Until this report, gene expression has not been explored to evaluate potential age-related, phenotypic consequences of *Ca. Liberibacter* infection of adult and nymphal psyllid stages. Understanding the genetic and biochemical mechanisms involved in the interplay between *Ca. Liberibacter* and the different life stages of the psyllid host is expected to provide clues about host-parasite co-evolution in

light of the need for host factors to be co-opted by *Liberibacter* essential for invasion-virulence, infection establishment and multiplication, systemic circulation, and *Liberibacter* persistence such that the bacterium is transmitted to its plant host.

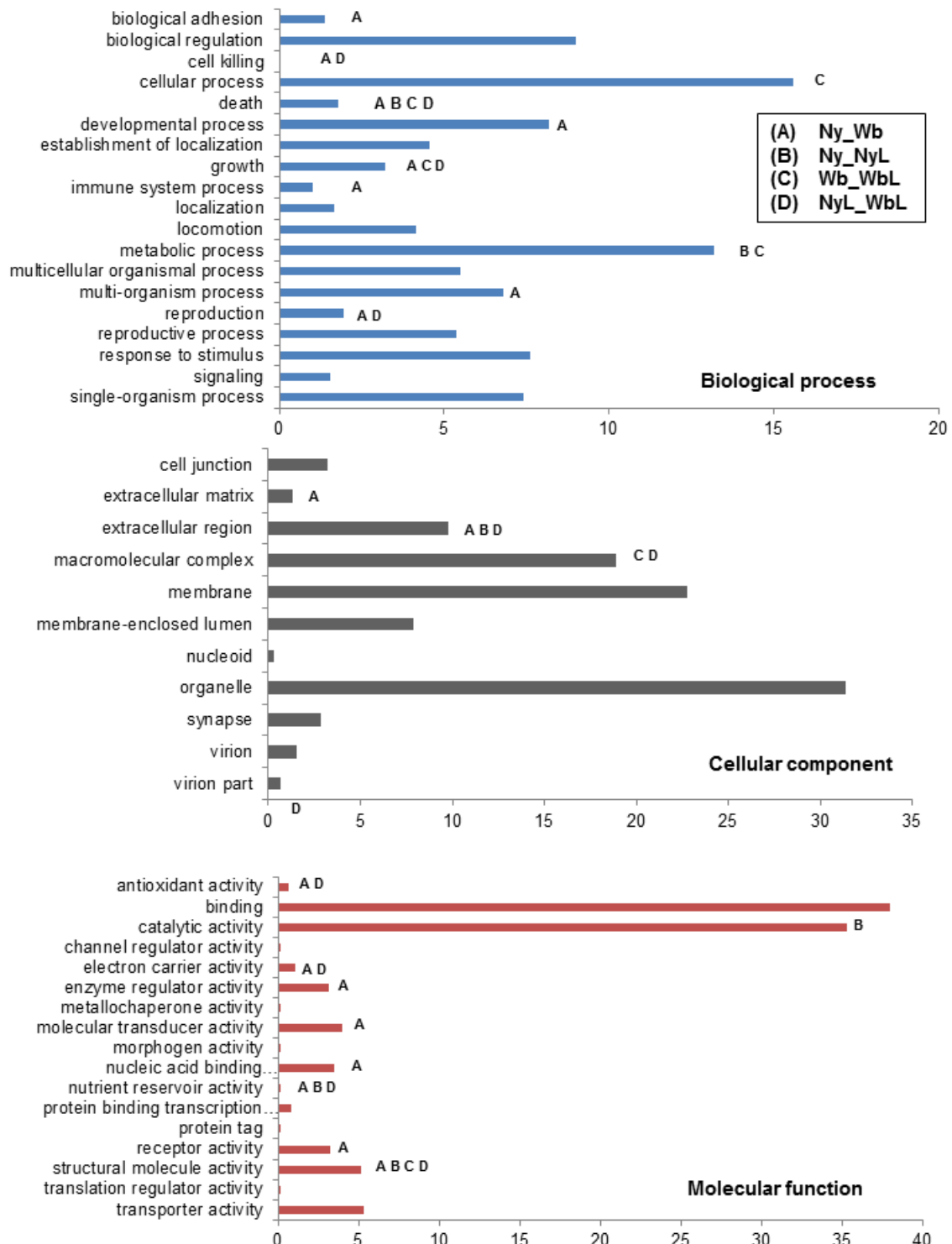
The Gene Ontology (GO) functional classification system [57] was used to classify PoP psyllid contigs for and among the different treatments (psyllid species, adults and nymphs, *Liberibacter* infection or *Liberibacter*-free). Forty-seven percent of PoP contigs (38,988) were represented by 50 functional groups (GO levels 1–2) (Figure 4). Among these 13,143 contigs were assigned to the biological process category, 11,969 were affiliated with cellular process, and 13,876 were assigned to molecular function. The ACP contigs (92%) were similarly distributed among the same three GO function categories [40]. Among the 47 PoP level 2 GO categories, 18 (38%) were identified as containing a significant number of differentially transcripts from comparisons of either uninfected adult *versus* nymph (Ny_Wb) or of infected adult *versus* nymph (NyL_WbL), underscoring the importance of life stage to the gene expression profile (Figure 4).

Here, significantly expressed transcripts were defined as those that had a *p*-value cut-off of 0.05 (using edgeR scoring [44]; Supplementary Tables S2–S5). Of 82,224 PoP transcripts, 3313 and 3533 transcripts were differentially expressed at 2-fold or greater with *p*-values <0.05 in response to CLso-infection in adults and nymphs, respectively (Supplementary Tables S2 and S3). Based on the main level 1 GO category assignments, most contigs had less than a 2-fold change in expression (Table 1). Approximately the same number of differentially expressed ACP and PoP transcripts was up- or down-regulated, however, the majority of down-regulated contigs belonged to PoP, while the up-regulated contigs were from ACP (Table 1). The differentially expressed contigs exhibiting a 2-fold or greater change in expression were correlated with *Liberibacter* infection, and/or to adult or nymph life stage, with life stage-associated altered expression being the most abundant (Table 1).

Table 1. Overall impact of *Candidatus Liberibacter*-infection on potato and Asian citrus psyllid adult and nymph contigs assigned to the level one Gene Ontology categories.

Expression Response	Biological Process				Cellular Process				Molecular Function			
	PoP		ACP		PoP		ACP		PoP		ACP	
	Adults	Nymphs	Adults	Nymphs	Adults	Nymphs	Adults	Nymphs	Adults	Nymphs	Adults	Nymphs
Up-regulated	7%	4%	14%	28%	7%	3%	14%	29%	9%	4%	14%	28%
Down-regulated	7%	14%	14%	11%	6%	14%	13%	11%	8%	17%	14%	11%
Unchanged	86%	82%	72%	61%	87%	83%	73%	60%	83%	79%	72%	61%

Figure 4. Differential expression of potato psyllid nymph and adult contigs within Gene Ontology categories. The potato psyllid transcripts could be assigned to 46 Gene Ontology functional classes. The x-axis indicates the percentage of contigs assigned to each class. The goseq statistical package was used to determine the assignments that contained an over-representation of differentially expressed contigs between treatments and indicated by a letter: pair wise comparison between PoP nymphs and adults (Ny/Wb; A), infected and uninfected nymphs (Ny/Ny; B), infected and uninfected adults (Wb/WbL; C) and infected nymphs and adults (NyL/WbL; D).



The most highly, differentially expressed PoP contigs that have predicted relevance to psyllid host-Liberibacter biological interactions were those related to biological adhesion, immune system processes, locomotion, and reproduction. Among these (Table 2) was a peritrophin-1, a chitin-binding protein found in the peritrophic matrix of insects, an important epithelial barrier to pathogen/parasite invasion [58,59]. Peritrophin-1 expression was found to be down regulated in CLso-infected nymphs (Supplementary Table S3), perhaps having the effect of increased vulnerability to invasion, compared to adults, resulting in the observation of lowered survivability of CLso-infected compared to -uninfected nymphs [19,20]. Further, among the 25 PoP contigs that exhibited the greatest differential expression in response to CLso infection (Table 2), 16% (4/25) were heat-shock-like proteins, and only a single such contig was found for PoP adults indicating that very different stress responses are stimulated by CLso infection in the psyllid life stages. In a parallel study of ACP adults and nymphs subjected to CLas infection, psyllid heat shock proteins were expressed to a greater level in the adults than in the immature stadia (Vyas *et al.* submitted 2014; see Supplementary Table S4). Taken together, we observed an inverse pattern of heat shock protein induction in adults and nymphs for both psyllid-Liberibacter pathogen complexes, a pattern that may be linked with reported stage-specific vector competence, *i.e.*, PoP adults and ACP nymphs, suggesting that the induction of heat shock proteins may be involved in CLso/CLas virulence, in that adults over nymphs are differentially susceptible to the pathogen. The intraspecies differences in life stage most influenced by Liberibacter infection provide robust evidence of distinct host- and Liberibacter-specific gene regulation patterns and underscore the importance of host life stage to Liberibacter parasitic strategies. These observations are consistent with the differential patterns of susceptibility of adults and nymphs to Liberibacter infection [11,16], and of unique host-parasite co-evolutionary relationships that characterize parasite adaptation, invasion, establishment and systemic infection of the different Liberibacter species [60,61].

2.2.1. Adhesion-Related Transcripts

Approximately 15% of all PoP contigs assigned to the biological adhesion category were significantly ($p < 0.05$), differentially expressed in adults and nymphs, with fold change ratios ranging from 3 to 300 times. Several highly differentially expressed contigs were annotated to chitin and cuticle proteins. Both of these protein types are known to be essential for insect growth and morphogenesis, and are involved in processes that modify chitin-containing structures [62]. The altered expression of adhesion-related contigs in PoP adults and nymphs could reflect an involvement in anatomical rearrangements during larval morphogenesis and adult gut epithelial renewal. Feasibly, proteins essential for adhesion-related physiological processes could influence transmission competency in adults and/or nymphs based on the expected requirement by Liberibacter to attach and persist.

For example, *Xyella fastidiosa* requires chitin localized in the mouthparts to colonize its homopteran insect host and vector [63]. The fastidious bacterial plant pathogen transmitted by *X. fastidiosa* differs from *Ca. Liberibacter* by being non-propagative and non-circulative in the vector, and, it systemically invades the plant host vascular system, mainly in the xylem. Because chitinolytic enzymes also can exhibit antibacterial properties [64] the “minimal” representation of immune pathway genes that encode antimicrobial peptides in insect vectors of fastidious, bacterial plant pathogens could reflect a protective mechanism of some kind, and if so could be involved in protection of bacterial

endosymbionts [25–30] or perhaps *Wolbachia*. Indeed this endochitinase was up-regulated 30-fold in *Liberibacter*-infected PoP nymphs (Supplementary Table S3).

Annexins are important for membrane organization and molecular trafficking [65]. Recent studies have demonstrated a role for an annexin in endocytosis-mediated-invasion [66] of insect peritrophic membranes and midgut epithelial cells by *Plasmodium* [67], resulting in loss of protection against parasitic invasion. In PoP an annexin-B9 transcript was up regulated 11-fold in the CLso-infected, compared to uninfected, nymphs and adults (Supplementary Tables S2 and S3), suggesting an unknown role in CLso virulence.

Table 2. The differentially expressed contigs for *Candidatus Liberibacter solanacearum*-infected and uninfected potato psyllid nymphs and adults, based on a *p*-value cutoff of 1E-6.

Nymph	Fold Change *	Adult	Fold Change *
Putative salivary protein	657.71	Cuticular protein 100A	49.29
Abdominal-B	91.35	Cuticular protein PpolCPR68	46.07
Cuticle protein 7	77.92	Putative ribosomal protein S13e	−23.42
Heat shock protein 70 A1	−120.68	Aconitate hydratase, mitochondrial	−120.89
Heat shock 70 kDa protein IV	−337.04	Cytochrome b561	17.63
Ubiquitin	−256.48	Senescence-associated protein, putative	19.59
60S ribosomal protein L5	−175.71	ATP synthase subunit alpha, mitochondrial	−109.49
Heat shock protein 70	−67.87	Arginine kinase	30.16
Putative ribosomal protein S13e	−69.98	60S ribosomal protein L5	−20.22
Probable RNA-directed DNA polymerase from transposon BS	−61.87	Endonuclease-reverse transcriptase	−96.94
Putative reverse transcriptase	−47.65	Ubiquitin	−25.09
FixR	26.65	Cathepsin D	−20.77
Translationally-controlled tumor protein homolog	−92.8	Reverse transcriptase-like protein	−27.8
Cathepsin B preproprotein-like protein	24.68	Meiotic recombination protein SPO11, putative	−21.61
Pyrroline-5-carboxylate dehydrogenase	−148.22	Protein painting of fourth	12.88
Vitellogenin	−40.34	Elongation factor 2	−23.81
Reverse transcriptase-like protein	−83.13	Phosphate carrier protein, mitochondrial	17.1
Putative small heat shock protein	−23.9	Retrovirus-related Pol polyprotein from transposon opus	11.87
SARTTc1 ORF2 protein	−29.89	Probable RNA-directed DNA polymerase from transposon BS	10.07
Tubulin alpha chain	−121.15	Cuticular protein 97Ea	9.96
Meiotic recombination protein SPO11, putative	−42.53	Enolase	−17.11
ATP synthase subunit alpha, mitochondrial	−25.5	F-element protein	−19.39
1-phosphatidylinositol-4,5-bisphosphate phosphodiesterase epsilon-1	11.15	Putative small heat shock protein	−15.97
Peritrophin-1, putative	−39.63	ATP-dependent RNA helicase p62	−14.72
Insecticide resistance protein CYP4G70	−96.66	Cathepsin B preproprotein-like protein	−11.99

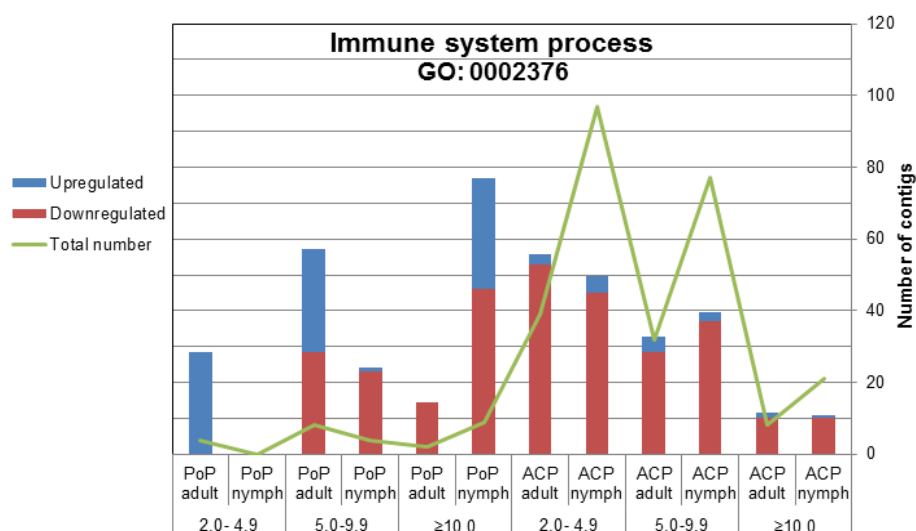
* Fold change value based on infected *versus* uninfected comparisons.

2.2.2. Immune System-Related Transcripts

The differential expression profiles together with gene ontological categorization of the PoP and ACP contigs revealed striking differences between the psyllid species. Among the total DE transcripts fewer than 1% of PoP contigs were immune-related, whereas, ACP had approximately 5%, and greater than 90% of these ACP immune-related DE contigs were down-regulated, compared to only 50% for PoP (Figure 5). Further, a greater number of immune-related contigs were differentially expressed in ACP nymphs compared to adults, and 92% were down regulated, pointing to a “weak” immune response by ACP nymphs to CLas invasion. Consistent with the above profiles, 62% of the immune-related DE contigs were down regulated in PoP nymphs, compared to 43% for adults, indicating a “weaker” immune response by PoP nymphs. Perhaps this suggests that CLas/CLso infection at the nymphal stage is a requirement for efficient adult-mediated bacterial transmission.

The innate immune system of some insects utilizes cell-mediated and humoral responses to pathogen invasion and attack [68], among which involve the synthesis of antimicrobial peptides usually through Toll and Immunodeficiency (IMD) pathways. These responses can result in melanin formation, and the stimulation of phagocytosis, and encapsulation. Psyllid counter attack to *Liberibacter* invasion and parasitism likely requires a competent immune system, while also balancing against hyper-immune expression that can potentially cause harm to the host and/or to its beneficial endosymbionts [69]. Indeed many bacteria, including *Ca. Liberibacter* form complex biofilms that provide protection from immune recognition [70–72], and studies in our lab have shown that CLso develops biofilms in and on PoP guts prior to circulation in the blood to reach the salivary glands [18].

Figure 5. Differential expression of immune-related contigs from the adult and nymphal stages of the potato and Asian citrus psyllid. The significantly differentially expressed potato and Asian citrus psyllid contig ($p > 0.05$; Ny/NyL, Wb/WbL) assignments to the Gene Ontology category Immune System Process (GO:0002376). Blue portion of bar indicates percentage of contigs that were up-regulated (*i.e.*, higher in infected psyllids) in response to *Ca. Liberibacter* infection. Red portion of bar indicates the percentage of contigs that were down-regulated (*i.e.*, lower in infected psyllids) in response to *Ca. Liberibacter* infection. The right x-axis denoted with green line indicates the number of contigs.



2.2.2.1. IMD Pathway

The (level 2) gene ontology-classified transcripts identified 907 PoP and 1226 ACP immune response transcripts, corroborating a previous report that the IMD pathway is suppressed in the potato psyllid [73]. Among these, two transcripts shared similarity with a caspase-1 protein (Supplementary Table S6). However, only caspase-8 homologs (*dredd*) are known to be components integral to the IMD pathway [74]. Caspases belong to a family of enzymes identified as effectors of apoptosis. Interestingly, two other transcripts shared similarity with an inhibitor of apoptosis-1, (IAP-1) and IAP-2 genes in the PoP transcriptome, pointing to inhibitory activity potentially directed at the IMD pathway (Supplementary Table S6). The IMD pathway responds to Gram-negative bacterial infection, however, it may not be capable of combatting Gram-negative bacteria like *Liberibacter* in a reduced state.

2.2.2.2. Toll Pathway

The Toll pathway is induced by gram-positive bacteria and fungi, and could be involved indirectly in the PoP-CLso pathosystem, perhaps through cell-mediated phagocytosis [75]. Transcripts that shared homology with all of the major protein components of the Toll pathway were identified in the psyllid transcriptome, some of which are *Toll*, *pelle*, *tube*, *cactus*, *dorsal*, *spätzle*, and *MyD88* homologs. The *Spätzle* homologs were significantly ($p < 0.05$) over expressed in uninfected nymphs compared to uninfected adults (Supplementary Table S4). However, the serine proteases required for *spätzle* activation *nudel*, *gd* (gastrulation defective), *snake*, and *easter* [76] were significantly down-regulated ($p < 0.05$) by 4- to 30-fold in the uninfected nymphs compared to uninfected adults (Supplementary Table S4), suggesting that nymphs are capable of a robust anti-bacterial response to gram-positive and fungal intruders, but later, may be less effective in combatting further invasion.

2.2.2.3. Phagocytosis

Profiles of the ACP and PoP immune-related contigs (significantly DE) responding to *Liberibacter* infection (Figure 5, Supplementary Table S6) reveal a number of proteins involved in phagocytosis. Classical phagocytosis is affiliated with pathogen-related innate immune responses, and serves as a first line of defense, as well as in tissue homeostasis and remodeling [77]. However, *Rickettsia* uses phagocytosis for epithelial cell entry [78]. Hijacking host factors to facilitate invasion is well documented among pathogenic bacteria [79,80], and underscores the potential for CLas/CLso exploitation of phagocytosis and possibly other exo-endocytic pathways of great interest. In this light, the expression of a diaphanous-like contig was found to be significantly reduced ($p = 0.0012$), at >19-fold in CLso infected PoP adults compared to nymphs (Supplementary Table S6). In a well-known pathosystem, the knockdown of diaphanous-1 (*Dia1*) interfered with *Rac-1* activation, which is required to trigger phagocytosis [81,82]. Additionally, *Rac-1* antagonism by a bacterial pathogen to maintain host cell viability that provides a permissive environment for the bacteria to replicate or evade host defenses has been shown [83]. The down-regulation of *Rac-1* could result in less efficient clearing of CLso from nymphs, compared to adults, and may implicate phagocytosis-like involvement in CLso invasion.

Two phagocytosis-inducing contigs; GTP-binding Di-Ras [84,85] and vacuolar protein sorting 16B (Vps16B) [86] were significantly up-regulated ($p < 0.05$) 5-fold in CLas-infected ACP adults compared to CLas-infected nymphs (Supplementary Table S6). Di-Ras, which stands for a distinct subgroup of Ras family proteins, are known to induce large cellular vacuolation in the host [84], a potentially critical step in pathogenesis. For example, the vacuolating cytotoxin (VacA) of *Helicobacter pylori* strains aid in uptake of *H. pylori* outer membrane vesicles (OMV) by host epithelial tissues [87]. Similarly, CLas may enhance ACP Di-Ras activity, in the less efficient host life stage, to promote epithelial cell death and/or apoptosis and increase cellular vacuolation to better facilitate dissemination in the psyllid.

Another phagocytosis related transcript (or contig) had similarity to a 1-phosphatidylinositol-4,5-bisphosphate phosphodiesterase epsilon-1 (PLCE-1) gene was 11-fold upregulated in CLso-infected PoP nymphs, but 4-fold down-regulated in CLas-infected ACP nymphs (Supplementary Table S6). PLCE-1 is a phosphoinositide-specific phospholipase C, an enzyme that enhances phagocytosis [88,89]. The opposing patterns of up and down regulation of PLCE-1 in PoP and ACP nymphs, respectively, suggest that the association of phagocytosis-related contigs with *Liberibacter* infection is important and warrants further investigation. For example, in ACP nymphs, the down-regulation of phagocytosis related transcripts may weaken the initial immune response. This could explain the greater susceptibility of this life stage to CLas invasion [16] and the higher rate of transmission compared to adults that were not exposed to CLas as nymphal instars [11].

2.2.3. Metabolic-Related Transcripts

The effect of *Liberibacter* on psyllid metabolic pathways was made evident from comparisons ($p < 10^{-5}$) of CLso-infected and uninfected PoP adults (Supplementary Table S8). This observation is not surprising since many bacteria have limited metabolic capabilities and rely on their host for energy precursors. For example, the branched chain amino acid biosynthetic pathways (to isoleucine, leucine and valine) are lacking in the CLso genome [90] and this may lead to host nutrient scavenging. Acyl-CoA dehydrogenases are mitochondrial flavoenzymes involved in fatty acid and chain amino-acid metabolism [91,92]. The greater than 19-fold reduction of an Acyl-CoA dehydrogenase-like contig in a psyllid may be associated with CLso's inability to carry out *de novo* synthesis of essential amino acids [90] and the psyllid response to prevent leaching thus suppressing bacterial growth.

Two contigs essential in the glycolysis and gluconeogenesis metabolic pathways were significantly ($p < 0.05$) down regulated in CLso infected nymphs compared to the uninfected (Supplementary Table S7). The first, an enolase-like contig was more than 80-fold decreased in CLso-infected nymphs. Enolases mediate immune evasion by degrading host tissues to prevent invasion [93] making its reduced expression potentially detrimental to CLso. The second gene, a phosphoglucomutase-like contig was 20-fold reduced (Supplementary Table S7), is implicated in lipopolysaccharide biosynthesis and biofilm formation [94,95], suggesting the psyllid down-regulates its glycolysis and gluconeogenesis to suppress bacterial invasion and multiplication.

Iron Metabolism

Iron regulation is known to be essential for successful entomopathogenic- and symbiotic bacterial interactions with insect host [96–98]. Data herein suggest that this scheme holds true for CLso as well, in that more than a third of the GO assignments that contained a significant number of differentially expressed contigs ($p < 1 \times 10^{-10}$) were involved in functions relating to ion regulation, with iron being the predominant ion (Supplementary Table S9). Ferritin is an iron storage and transport protein important for antioxidation and detoxification [99], and the iron transporter, transferrin, has antioxidant properties to combat invasion by pathogens and parasites [100]. Both of these contigs were significantly up regulated in CLso-infected adults and less so in CLso-infected nymphs (Supplementary Table S10), indicating that iron is essential for CLso pathogenesis of PoP, and therefore a potentially lucrative target for RNAi.

2.3. Orthologs in the Potato and Asian Citrus Psyllid Transcriptomes

We explored orthologs, or groups of genes that are similar in sequence, structure, domain architecture and function [101] to identify relevant biological functions central to ACP and PoP, as related psyllid species. Also of interest were species specific differences in physiological and metabolic adaptation that could illuminate evolutionary and functional conservation of host-pathogen interactions in a circulative, propagative mode of transmission. The ACP and PoP transcriptomes include all contigs in CLso/CLas-infected and -uninfected adults and nymphs that are potentially involved in host-pathogen interactions. Coding regions in the PoP and ACP contigs were identified using ESTscan [102], available in the TCW, and these were submitted OrthoMCL clustering [103], also available in the TCW, to identify orthologous genes (contigs).

Using this approach, it was possible to identify coding regions in 57% and 41% of the ACP and PoP contigs, respectively, totaling 60,085 coding sequences (CDS) of which 67% were assignable to 8721 orthologous groups or clusters (Supplementary Table S11) using OrthoMCL default parameters (1.5 inflation value; 103). Clusters ranged from 2 to 285 CDSs in size those containing 5 or more clusters predominating (Figure 6). The OrthoMCL-defined orthologous groups include one-taxon multicopy ($1 \times N$), two-taxon single copy (2×1), and two-taxon multicopy ($2 \times N$) groups representing paralogous (one-taxon) and orthologous (two-taxon) gene families.

Also, the RPKM value of each sequence (CDS) pair per cluster was compared using the Pearson Correlation Coefficient (PCC) [104], an average value was calculated for each cluster (perPCC) so that they could be filtered based on percentages of pairs having a PCC value of ≥ 0.8 . The perPCC [105] value provides a statistical indication of the extent to which the contig expression is synchronized within a cluster. The results indicated that ACP and PoP contig expression profiles were distinct (Figure 7), despite sharing a large number of genes in common. This might have been expected given distinct host range, different environmental niche, and transmission phenotypes associated with the adult and nymph life stages. The perPCC values ranged from 35% to 42% within the single-taxon groups, but decreased to 8%–18% when both PoP and ACP were included (two-taxon; Figure 7).

Figure 6. Classification of Asian citrus and potato psyllid contigs into orthologous groups and clustering of transcripts. (A) Numbers of orthologous groups detected across the two species with OrthoMCL. The one-taxon groups ($1 \times N$) are unique to each psyllid species. Two-taxon are found in both and are categorized as single copy (2×1 ; red letters) and multicopy ($2 \times N$; black letters).

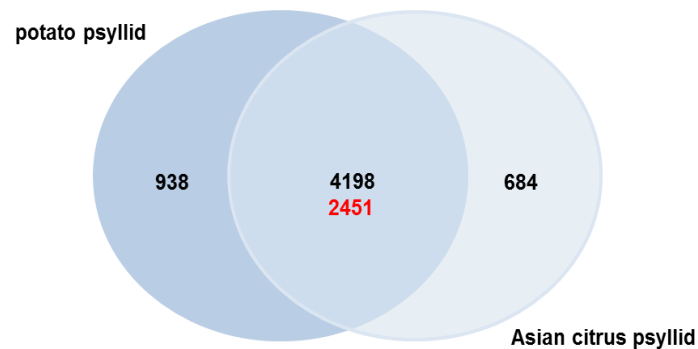
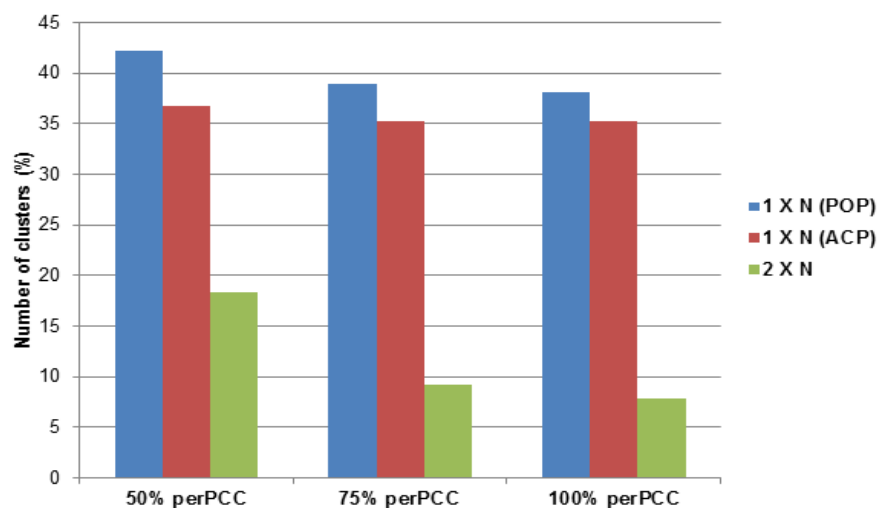


Figure 7. Analysis of OrthoMCL multicopy cluster member expression. Expression (*i.e.*, RPKM-reads per kilobase per million) values of each sequence pair in a cluster were compared for their Pearson Correlation Coefficient (PCC). Graph shows percent of pairs per cluster with PCC values ≥ 0.8 (y-axis) versus percentage of total number of clusters in the category (x-axis). Single taxon groups ($1 \times N$) contained more clusters of uniformly expressed contigs ($\geq 50\%$ perPCC in comparison to two-taxon groups ($2 \times N$).



2.3.1. Potato Psyllid Paralogous Gene Families

In PoP, 15% of the CDSs were assigned to single-taxon clusters. One such set was containing four members coding for *trans*-sialidase-like proteins. Sialidases are glycosylhydrolases that can contribute to the provision of free sialic acid [106]. Sialic acid is synthesized *de novo* by bacteria or scavenged from the host as a protective covering, providing protection from innate host immunity or used as a nutrient source [107]. Expression of these contigs was at near steady state levels in PoP adults, but was more than 3-fold down-regulated in nymphs in response to *Liberibacter* infection (Supplementary Table S12). The reduced expression in infected nymphs could be the result of the immature psyllid

host's efforts to reduce pathogen presence by eliminating protective or nutritive resources potentially vital for CLso survival. Another group shared amino acid sequence similarity to a hemolysin-E gene (*hlyE*). These hemolysin-E like contigs are present in both CLso-infected and-uninfected psyllids, indicating that they are of psyllid origin, or they represent carry over during isolation procedures of transcripts for PoP endosymbionts. HlyE is a novel pore-forming toxin produced by *Escherichia coli*, is distinct from the well-characterized pore-forming *E. coli* hemolysins [108], and in the presence of lipids forms transmembrane pores in small intestine epithelial cells [109]. A similar pore-forming toxin was characterized from the kissing bug, *Triatoma infestans*, which showed both antimicrobial and lytic activity towards *Trypanosoma cruzi* and human cells [110]. Only one of the nine HlyE-like contigs in this group showed significant expression changes with a 14-fold increase in expression in infected compared to uninfected PoP adults (Supplementary Table S12), likely indicating an antibacterial role. However, CLso may utilize the pore-forming activity to invade or to escape.

2.3.2. Asian Citrus Psyllid Paralogous Gene Families

In ACP, 9% of the CDSs were assigned to single-taxon clusters. Several may be putatively involved in host-pathogen interactions. This includes a three-member group of contigs with similarity to the haematopoietic transcription factor *serpent*, a known regulator of insect immunity [111]. These were detected in both CLas-infected and -uninfected ACP and overall expression was reduced in CLas-infected ACP adults and nymphs (Supplementary Table S11).

Cluster analysis also showed that adult and nymph ACP have an additional calpain family member, compared to PoP adults and nymph (Supplementary Table S11). Calpains are a large family of calcium-regulated cytosolic cysteine peptidases involved in many cellular processes, including the rearrangement of cytoskeletal proteins, signal transduction pathways, and in apoptosis by catalyzing the controlled proteolysis of targeted proteins [112].

2.3.3. Asian Citrus and Potato Psyllid Orthologous Gene Families

Even though ACP is oligophagous [113] it feeds primarily on species in the Rutaceae, and transmits three citrus-infecting *Ca. Liberibacter* species, while PoP is polyphagous on a wide range of solanaceous as well as other plant species [1], and specifically transmits CLso, the majority (91% and 85% for ACP and PoP, respectively) of the CDSs identified were detected in both psyllid species (at 2×1 and $2 \times N$), suggesting that these two psyllid species harboring different *Liberibacter* are nonetheless similar at the amino acid (protein) level.

To identify gene families common to both psyllids with potentially conserved biological relevance to psyllid biology and/or *Liberibacter* transmission, filtering was also carried out using more stringent constraints than those set by the default parameters of the software, requiring at least 80% overlap and 80% sequence similarity among the OrthoMCL-defined groups. The analysis yielded 4836 orthologous groups that contained 2 to 43 CDSs, and reduced the number of $2 \times N$ groups by ~90% to 458 (Supplementary Table S13) due to the exclusion of less functionally similar orthologs. Further, only 9% of the clusters in the $2 \times N$ groups had PCC values ≥ 0.8 (Table 3), underscoring the variability of expression profiles of the two psyllids. In light of this, identifying the commonalities shared between

the ACP and PoP could be instrumental in illuminating conserved host-pathogen proteins and mechanisms involved in circulative, propagative transmission.

Table 3. List of top two-taxon multicopy OrthoMCL groups found in the potato and Asian citrus psyllid transcriptomes, including group size, description (UniProt), and Pearson Correlation Coefficient values.

Cluster ID	Size	Description	perPCC
TR_000786	3	3-hydroxy-3-methylglutaryl-coenzyme A reductase	100
TR_003785	3	Abc transporter	100
TR_000835	3	Atlastin	100
TR_001975	3	Calmodulin	100
TR_001355	3	cAMP-dependent protein kinase catalytic subunit, putative	100
TR_000708	4	Chitin synthase 1 variant b	100
TR_000290	3	Cleavage and polyadenylation specificity factor subunit 1	100
TR_001473	3	Cytochrome P450, putative	100
TR_000343	4	DNA replication licensing factor MCM4	100
TR_000489	3	DNA-binding protein Ewg, putative	100
TR_001764	3	Dual oxidase maturation factor 1	100
TR_000565	3	Dynamin-like 120 kDa protein, mitochondrial	100
TR_000908	3	E78 nuclear receptor	100
TR_000324	3	EH domain-binding protein 1	100
TR_000905	3	F-box only protein, putative	100
TR_000639	3	Forkhead box protein K1	100
TR_000486	3	Hedgehog protein	100
TR_000141	3	Inactive ubiquitin carboxyl-terminal hydrolase 54	100
TR_000345	3	Kinesin-like protein KIF21B	100
TR_000433	3	Merlin	100
TR_001523	3	Mitogen-activated protein kinase ERK-A, putative	100
TR_000402	3	Phosphatidylserine synthase 1	100
TR_002280	4	Probable aconitate hydratase, mitochondrial	100
TR_000043	3	Probable phosphorylase b kinase regulatory subunit alpha	100
TR_000068	4	Probable pre-mRNA-splicing factor ATP-dependent RNA helicase mog-5	100
TR_000493	3	Protein turtle	100
TR_000691	3	Protein Wnt	100
TR_000597	3	Proton-coupled amino acid transporter 4	100
TR_001033	3	Putative AMP dependent CoA ligase	100
TR_000510	3	Pyruvate dehydrogenase E1 component subunit beta, mitochondrial	100
TR_000027	3	SH3 and multiple ankyrin repeat domains protein 3	100
TR_001667	3	Shc transforming protein, putative	100
TR_001186	3	Techylectin-5B	100
TR_000532	3	Transient receptor potential cation channel trpm	100
TR_000454	3	Triacylglycerol lipase, pancreatic, putative	100
TR_000971	4	Actin-binding protein IPP	83.33
TR_001171	4	Putative GPCR-type octopamine beta receptor (Fragment)	83.33
TR_000754	4	Sodium/hydrogen exchanger	83.33
TR_000042	4	Tyrosine-protein kinase transforming protein FPS, putative	83.33
TR_000375	5	Ephrin receptor	80

Nipah and Hendra viruses (*Henipavirus*) enter mammalian host endothelial cells by attachment to the ephrin-B2 and/or -B3 receptors [114]. A five-member $2 \times N$ group sharing an interesting similarity with the Ephrin-like receptors, were down-regulated in response to CLAs and CLso, suggesting these genes could be involved in bacterial invasion of psyllid gut and/or salivary gland tissues. Another $2 \times N$ group that contained three-members showed similarity with transient receptor-potential proteins (Supplementary Table S13), which are a multigene superfamily of integral membrane ion channel proteins that participate in diverse physiological processes, including sensing stimuli and ion homeostasis [115]. A three member $2 \times N$ group coding techylectin-like immune proteins (Supplementary Table S13), were differentially expressed in CLAs/CLso infected adults and nymphs. These kinds of proteins are known to have a role in phagocytosis and participate either by responding to immune defenses [116,117], and/or in host cell membrane invasion. Based on the *in silico* identification of several phagocytosis-related proteins in the ACP and PoP transcriptomes, *Liberibacter* may interact with them as well as techylectin-like proteins as a common mechanism for psyllid cell entry during invasion. Two additional contigs identified by cluster analysis with a possible role in host-pathogen interactions were phosphatidylserine synthase 1 and triacylglycerol lipase (three members, each) (Supplementary Table S13), enzymes involved in sphingolipid and/or phospholipid metabolism [118,119]. These enzymes are not produced by the majority of bacteria but many use host sphingolipids as cell-surface protectants for evading host immune responses, to facilitate colonization [118], and perhaps in biofilm formation [120].

3. Methods

3.1. Psyllids

Ca. *Liberibacter solanacearum* (CLso) -infected psyllids were collected from a psyllid-infested tomatoes from a greenhouse in Arizona in 2004 and maintained as a laboratory colony at the University of Arizona since then. CLso-infected psyllids were reared on tomato plants (Roma) under laboratory conditions with temperature of ~ 24 °C and a photoperiod of 12:12 h (light and dark) and transferred serially to fresh plants approximately every 3–5 weeks. The CLso-free (uninfected) potato psyllids were obtained from Dr. J. Munyaneza. Psyllids were haplotyped as the “central-type” using the cytochrome oxidase I gene as a molecular marker [121] and colonies were routinely checked for CLso presence or absence by PCR using primers that amplify the 16S rRNA gene [3,122]. Adult and nymphs (2–5 instar) were collected so that the most complete whole transcriptome data set could be generated over a complete range of adult and nymph life stages representing complete cohorts minus the first instar, which was too small to obtain near-equal body weight in comparison to the other nymphal instars. Live psyllids were collected from the colonies and subjected to processing by crushing lightly in RNA-free tubes by micro-pestles, followed by the addition of Trizol (Invitrogen, Carlsbad, CA, USA), prior to overnight shipping on dry ice to Washington State University (WSU) where they were stored at -80 °C until total RNA was isolated. The CLAs-infected and -uninfected ACP colonies were reared in laboratory cultures maintained on a CLAs host (*Citrus* spp.) or a CLAs- immune rutaceous plant species. Cultures were reared continuously and serially transferred periodically to the same host species at the University of Florida Citrus Research and Education Center

(courtesy, Dr. K.S. Pelz-Stelinski, Lake Alfred, FL, USA) or at the Southwest Florida Research and Education Center (courtesy, Dr. P.A. Stansly, Immokalee, FL, USA). Adults and nymphs (2–5 instar) were collected and processed in the same manner as described above for PoP and the RNA samples were also shipped to WSU where they were stored at $-80\text{ }^{\circ}\text{C}$ until use. ACP transcripts used for comparative analyses in this study were obtained in a similar fashion as described below for PoP and in a simultaneously submitted manuscript [40].

3.2. RNA Isolation and Quality Control

Total RNA was isolated from 225 to 250 adult or nymph psyllids either infected or uninfected with *Candidatus Liberibacter solanacearum*. Previously crushed psyllid samples were supplied in 1 mL Trizol each. For RNA extraction, 0.3 mL chloroform were added to 1 mL Trizol homogenate, followed by vigorous sample shaking for 30 s, and incubation for 3 min at room temperature. The samples were centrifuged at $12,000 \times g$ for 15 min at $4\text{ }^{\circ}\text{C}$ to separate the organic from the aqueous phase. The aqueous phase (200–250 μL) was transferred to a new, sterile RNase-free tube and an equal volume of 100% EtOH was added, with mixing. Samples were further purified using the RNeasy Mini Kit (Qiagen, Valencia, CA, USA) according to the manufacturer's protocol. The quality and quantity of each RNA sample was assessed using a NanoDrop 2000 Spectrophotometer (Thermo Scientific, Wilmington, DE, USA) with A260:A280 ratio greater than 2.0. RNA integrity was confirmed using an Agilent 2100 Bioanalyzer (Agilent Technologies Inc., Santa Clara, CA, USA) with an RNA Integrity Number (RIN) value greater than or equal to 8.

3.3. Library Construction and Illumina Paired-End Sequencing

The poly(A) RNA was isolated from 2 μg of total psyllid RNA from each treatment using magnetic oligo (dT) beads. Following purification, the mRNA was fragmented by zinc treatment at $94\text{ }^{\circ}\text{C}$ for 5 min and reverse-transcribed to synthesize first strand cDNA using SuperScript II reverse transcriptase (Invitrogen) and random primers, followed by second-strand cDNA synthesis. The cDNAs were subjected to end-repair and phosphorylation and the addition of an "A" base to the 3'-end of the blunt phosphorylated DNA fragments. Illumina Paired-End (PE) adapters were ligated to the fragments, as described by Illumina's Paired-End Sample Preparation Guide (Illumina). A 250 bp ± 25 bp smear containing the cDNA fragments, flanked by Illumina PE adapters, was cut from a 2% agarose gel for downstream enrichment. The cDNA fragments were amplified by PCR Primers PE 1.0 and PE 2.0 (Illumina) that anneal to the ends of the adapters, using the PCR program of 30 s at $98\text{ }^{\circ}\text{C}$ followed by 15 cycles of 10 s at $98\text{ }^{\circ}\text{C}$, 30 s at $60\text{ }^{\circ}\text{C}$, 15 s at $72\text{ }^{\circ}\text{C}$ and a final elongation step of 5 min at $72\text{ }^{\circ}\text{C}$. The products were purified using the QIAquick PCR Purification Kit (Qiagen) to create an Illumina paired-end library for each treatment. Library quality control was performed with a Bioanalyzer DNA 1000 Chip Series II (Agilent). A qPCR method was employed to quantify libraries in advance of generating clusters. The libraries were diluted to a final concentration of 10 nM. The paired-end libraries were applied for cluster generation at a concentration of 10 pM in a flowcell on a cBOT (Illumina). Sequencing was performed with one lane per library of 2×54 bp reads from both ends of the fragments on an Illumina Genome Analyzer Iix at the National Center for Genome

Resources (NCGR). The complete dataset has been deposited to the Short Read Archive (SRA) at GenBank, under accession PRJNA252003, SRX583042, and SRX583048.

3.4. Assembly, Annotation and Comparison of Illumina Sequences

The Illumina reads were cleaned and assembled as described in He *et al.* 2010 [123]. Briefly, the reads were assembled with ABySS [124], the gaps were filled used GapCloser in SOAP [125], the scaffolds merged with Mira [126] and filtered for redundancies with CD-HIT [127], and the reads were aligned *post hoc* to the final contig consensus sequences using Burrows-Wheeler Alignment (BWA) [128].

The resulting transcripts and read counts were loaded into Transcriptome Computational Workbench (TCW) [39], where the transcripts were annotated using an E-value cutoff of 10^{-10} against a subset of the UniProt taxonomic databases [46,47] and the GO terms extracted from the “.dat” files [57]. Based on the TCW, levels of significance of differentially expressed transcripts for individual and those grouped in GO categories were determined by edgeR [44] and goseq [129] analysis, respectively. These results were analyzed with the TCW interactive Java interface, publicly available at www.sohomoptera.org. The results for the figures and tables were created using either the TCW software for single (sTCW) or multiple (mTCW) database comparisons. The results shown in Table 1 were obtained using the “include” and “exclude” filter for the libraries of interest selected with minimum 2-fold up and down option for each level 1 GO category (biological process GO: 0008150, cellular component GO: 0005575 and molecular function GO: 0003674). The sum of up and down changes was subtracted from total number of transcripts and expressed as a percent. The results shown in Table 2 and Supplementary Tables S2–S5 were obtained by using the “include” and “exclude” filter for the libraries of interest selected having the differential expression value cutoff of 0.05. The results summarized in Figure 4 were obtained with the “Basic GO Query” with filters set to view level 2 GOs with a differential expression *p*-value threshold of 0.05 for all libraries. The results Supplementary Tables S6–S10 were obtained by selecting “to show” transcripts with reads from all libraries, and all GO levels, either grouped (Table 3) or not grouped by GOs (Supplementary Tables S6–S10). Significance of differential expression was based on either a *p*-value cutoff of 10^{-5} or 10^{-10} , with stringency selection based on the results obtained using each method. The results in Table 3 and Supplementary Tables S12–S13 were obtained within TCW using the “transitive” option for cluster analysis, showing all two-taxon multicopy ($2 \times N$) clusters having at least 80% of pairs having Pearson Correlation Coefficient (PCC) value ≥ 0.8 .

The TCW executed the ESTScan software [102] on the transcripts to identify peptides with a minimum cutoff of 30 amino acids, using a training matrix produced from the Hemiptera proteins from GenBank. The TCW was used to execute the OrthoMCL software [103] to compute ortholog clusters from these two peptide sets using an inflation parameter of 1.5 to balance sensitivity with selectivity. The orthologous groups were combined in TCW with the annotation and expression levels from the individual TCW databases. Finally, the majority UniProt hit was assigned to each group. The results in Supplementary Tables S11–S12 were obtained using default parameters, showing all clusters.

3.5. Transmission Electron Microscopy

For negative staining, CLso-infected and uninfected adults were vortexed in 5% bleach 10 s, and midguts were extirpated in diethyl pyrocarbonate (DEPC) treated H₂O. Each was transferred to individual pioloform coated grids containing 20 µL of DEPC H₂O. Five minutes after gentle mastication with insect pins, tissue fragments were removed, and the hemolymph/water solution was allowed to evaporate to a thin film before the addition of 2.5 µL 4% glutaraldehyde. Specimens were fixed 10 min. One drop (~10 µL) of 2% uranyl acetate was added and allowed to stand for 2 min, followed by blotting with filter paper and air-drying. The grid was air-dried for several hours and examined using a Phillips CM-12 transmission electron microscope operated at 80 kV.

4. Conclusions

This manuscript highlights the results of an interdisciplinary research effort that has produced the first annotated, differentially expressed transcriptomes of adult and nymphal stage PoP either free of or harboring CLso. This PoP transcriptome database contains 82,224 contigs, of which 16,496 (20%) could be annotated. The availability of the psyllid (PoP and ACP) annotated transcriptome database integrated with comparative profiling and search tools offers a novel opportunity to exploit new knowledge about host-parasite interactions in this pathosystem. Impressive differences in the expression levels of the same or similar contigs occurred for ACP and PoP adults and nymphs infected or uninfected with *Liberibacter*, suggesting some extent of host-parasite co-evolution, despite the different host insects and *Liberibacter* pathogen species involved. It is anticipated that functional studies for protein and gene families common to both psyllid species, now in progress, will lead to discoveries of evolutionarily conserved genes important in host-parasite interactions to enhance our knowledge of psyllid biology, as well as those involved in conserved host-parasite interactions across hemipteran insects.

The linked cluster analysis software facilitates the identification of psyllid species- and life stage-specific proteins, and gene families shared across two psyllid species. The close parasitic relationships only recently recognized between certain psyllid species and the genus *Ca. Liberibacter* will make it possible to consider networks of psyllid proteins from similar and different gene families that interact with *Liberibacter* proteins to further illuminate co-evolutionary relationships involving both parasitic or symbiotic outcomes.

The *in silico* annotated transcriptomes and differential expression profiling of the different life stages of PoP and ACP harboring CLso have produced a lucrative list of effector targets that may serve as determinants of infection, multiplication, circulation and the acquisition process in two different psyllid-*Liberibacter* study systems. For example, a putative psyllid annexin- and an ephrin receptor-like contigs were identified that may be required for bacterial invasion. Also this list includes many endocytosis-related genes such as a Vps16B and Di-Ras, initially assumed to be involved in phagocytic psyllid immune responses but may be advantageously used by CLas/CLso to gain entry into its host. Metabolic and nutritionally directed investigations led to the addition of enolase- and transferrin-like psyllid genes to this list, both potentially having an effect on CLas/CLso virulence capabilities. Lastly, the *in silico* identification (this study) and subsequent TEM and RT-PCR

validation of expressed flagellar- and pilus-like structures adds target effector(s), which may be involved in bacterial persistence and/or dissemination in psyllids, to this list. Functional validation and biochemical characterization of the remaining most promising effector targets are ongoing, and preliminary data suggests significant advancements in our goal of targeting effectors that interfere with psyllid-mediated circulative, propagative transmission of *Liberibacter* becoming a reality.

The abundance of predicted protein interactors having putative CLso effectors encoded by PoP and ACP nymphs and adults underscore the apparent abundance of direct and indirect psyllid responses to *Liberibacter* infection, providing evidence of conserved mechanisms in psyllid-*Liberibacter* interactions. These proteins are cataloged in linked databases to allow for comparative data mining using the ACP/PoP website, and provide a valuable, user-friendly, comprehensive molecular and bioinformatics resources to advance research in potato and Asian citrus psyllid biology, genetics, and functional genomics.

Of particular interest to our efforts are those effector-interactor pairs with pivotal functions in modulating CLAs/CLso-psyllid interactions. Examples of these are psyllid proteins that interact with bacterial effectors to mediate virulence, adherence, entry-invasion, nutritional exploitation, evasion of host immunity, and persistence and circulation in psyllid host tissues. Our hope is that these tools will serve as a relevant starting point to guide RNA-interference strategies for abatement of psyllid-mediated *Liberibacter* transmission, with an immediate and timely emphasis toward managing citrus greening disease.

Acknowledgments

The authors wish to thank all of our colleagues in the laboratory who assisted in aspects of colony maintenance and molecular assays, in particular Della Carbonaro. We also thank Joseph E. Munyaneza, USDA-ARS, Yakima, WA for generously providing CLso-free PoP psyllids used in this study. This research was funded by the Citrus Research and Development Foundation (CRDF), Lake Alfred, FL, USA.

Author Contributions

TF and MV carried out the analysis and interpretation of data and drafted the manuscript. RH was involved in construction of the transcriptome libraries and participated in data analysis. CS and WN annotated the libraries, carried out all bioinformatics analysis, and designed the software and website. JMC collected and processed insects for the library construction and performed transmission electron microscopy analysis. Ryan Kim, Robin Kramer, GM and JC were involved in sequencing of the transcriptome library. DG, CS, and JKB collaborated in conception of the study and the website content, and in writing and editing the manuscript. All authors have read and approved the submission.

Abbreviations

ACP	Asian citrus psyllid
CLas	<i>Candidatus Liberibacter asiaticus</i>
CLso	<i>Candidatus Liberibacter solanacearum</i>
GO	Gene Ontology

HLB	Huanglongbing
PCC	Pearson Correlation Coefficient
perPCC	average PCC per cluster
PoP	potato psyllid
RPKM	<i>Reads per KB per million reads</i>
ZC	Zebra chip disease

Conflicts of Interests

The authors declare no conflict of interest.

References and Notes

- Munyaneza, J.E. Psyllids as vectors of emerging bacterial diseases of annual crops. *Southwest. Entomol.* **2010**, *35*, 471–477.
- Brown, J.K.; Rehman, M.; Rogan, D.; Martin, R.R.; Idris, A.M. First Report of “*Candidatus Liberibacter psyllaourous*” (synonym “*Ca. L. solanacearum*”) Associated with “Tomato Vein-Greening” and “Tomato Psyllid Yellows” Diseases in Commercial Greenhouses in Arizona. *Plant Dis.* **2010**, *94*, 376–376.
- Liefting, L.W.; Sutherland, P.W.; Ward, L.I.; Paice, K.L.; Weir, B.S.; Clover, G.R. G. A New “*Candidatus Liberibacter*” Species Associated with Diseases of Solanaceous Crops. *Plant Dis.* **2009**, *93*, 208–214.
- Hansen, A.K.; Trumble, J.T.; Stouthamer, R.; Paine, T.D. A new Huanglongbing Species, “*Candidatus Liberibacter psyllaourous*”, found to infect tomato and potato, is vectored by the psyllid *Bactericera cockerelli* (Sulc). *Appl. Environ. Microbiol.* **2008**, *74*, 5862–5865.
- Crosslin, J.M.; Munyaneza, J.E.; Brown, J.K.; Liefting, L.W. A history in the making: Potato zebra chip disease associated with a new psyllid-borne bacterium—A tale of striped potatoes. *APSnet Feature* **2010**, doi:10.1094/apsnetfeature-2010-0110.
- Sengoda, V.G.; Munyaneza, J.E.; Crosslin, J.M.; Buchman, J.L.; Pappu, H.R. Phenotypic and etiological differences between psyllid yellows and zebra chip diseases of potato. *Am. J. Potato Res.* **2010**, *87*, 41–49.
- Gottwald, T.R. Current Epidemiological Understanding of Citrus Huanglongbing. *Annu. Rev. Phytopathol.* **2010**, *48*, 119–139.
- Duan, Y.; Zhou, L.; Hall, D.G.; Li, W.; Doddapaneni, H.; Lin, H.; Liu, L.; Vahling, C.M.; Gabriel, D.W.; Williams, K.P.; Dickerman, A.; Sun, Y.; Gottwald, T. Complete genome sequence of citrus huanglongbing bacterium, “*Candidatus Liberibacter asiaticus*” obtained through metagenomics. *Mol. Plant Microbe Interact.* **2009**, *22*, 1011–1020.
- Lin, H.; Gudmestad, N.C. Aspects of Pathogen Genomics, Diversity, Epidemiology, Vector Dynamics, and Disease Management for a Newly Emerged Disease of Potato: Zebra Chip. *Phytopathology* **2013**, *103*, 524–537.
- Jagoueix, S.; Bove, J.; Garnier, M. The phloem-limited bacterium of greening disease of citrus is a member of the α subdivision of the Proteobacteria. *Int. J. Syst. Bacteriol.* **1994**, *44*, 379–386.

11. Inoue, H.; Ohnishi, J.; Ito, T.; Tomimura, K.; Miyata, S.; Iwanami, T.; Ashihara, W. Enhanced proliferation and efficient transmission of *Candidatus Liberibacter asiaticus* by *adult Diaphorina citri* after acquisition feeding in the nymphal stage. *Ann. Appl. Biol.* **2009**, *155*, 29–36.
12. Ammar, E.; Shatters, R.G., Jr.; Hall, D.G. Localization of *Candidatus Liberibacter asiaticus*, Associated with Citrus Huanglongbing Disease, in its Psyllid Vector using Fluorescence *in situ* Hybridization. *J. Phytopathol.* **2011**, *159*, 726–734.
13. Ammar, E.; Shatters, R.G., Jr.; Lynch, C.; Hall, D.G. Detection and Relative Titer of *Candidatus Liberibacter asiaticus* in the Salivary Glands and Alimentary Canal of *Diaphorina citri* (Hemiptera: Psyllidae) Vector of Citrus Huanglongbing Disease. *Ann. Entomol. Soc. Am.* **2011**, *104*, 526–533.
14. Sengoda, V.G.; Buchman, J.L.; Henne, D.C.; Pappu, H.R.; Munyaneza, J.E. “*Candidatus Liberibacter solanacearum*” Titer Over Time in *Bactericera cockerelli* (Hemiptera: Triozidae) after Acquisition from Infected Potato and Tomato Plants. *J. Econ. Entomol.* **2013**, *106*, 1964–1972.
15. Cooper, W.; Sengoda, V.; Munyaneza, J. Localization of “*Candidatus Liberibacter solanacearum*” in *Bactericera cockerelli* (Hemiptera: Triozidae). *Ann. Entomol. Soc. Am.* **2014**, *107*, 204–210.
16. Pelz-Stelinski, K.S.; Brlansky, R.H.; Ebert, T.A.; Rogers, M.E. Transmission parameters for *Candidatus liberibacter asiaticus* by Asian citrus psyllid (Hemiptera: Psyllidae). *J. Econ. Entomol.* **2010**, *103*, 1531–1541.
17. Mann, R.S.; Pelz-Stelinski, K.; Hermann, S.L.; Tiwari, S.; Stelinski, L.L. Sexual transmission of a plant pathogenic bacterium, *Candidatus Liberibacter asiaticus*, between conspecific insect vectors during mating. *PLoS One* **2011**, *6*, e29197.
18. Cicero, J.M.; Fisher, T.W.; Stansly, P.A.; Brown, J.K. are preparing the manuscript with title “Anatomical evidence for circulation and propagation of *Candidatus Liberibacter solanacearum* in the potato psyllid vector, *Bactericera cockerelli* (Sulc) (Hemiptera: Triozidae)” 2014.
19. Nachappa, P.; Levy, J.; Pierson, E.; Tamborindegy, C. Correlation between “*Candidatus Liberibacter solanacearum*” infection levels and fecundity in its psyllid vector. *J. Invertebr. Pathol.* **2013**, *115*, 55–61.
20. Nachappa, P.; Shapiro, A.A.; Tamborindegy, C. Effect of “*Candidatus Liberibacter solanacearum*” on Fitness of Its Insect Vector, *Bactericera cockerelli* (Hemiptera: Triozidae), on Tomato. *Phytopathology* **2012**, *102*, 41–46.
21. Thao, M.L.; Clark, M.A.; Burckhardt, D.H.; Moran, N.A.; Baumann, P. Phylogenetic analysis of vertically transmitted psyllid endosymbionts (*Candidatus Carsonella ruddii*) based on *atpAGD* and *rpoC*: Comparisons with 16S–23S rDNA-derived phylogeny. *Curr. Microbiol.* **2001**, *42*, 419–421.
22. Nachappa, P.; Levy, J.; Pierson, E.; Tamborindegy, C. Diversity of endosymbionts in the potato psyllid, *Bactericera cockerelli* (Trioziidae), vector of zebra chip disease of potato. *Curr. Microbiol.* **2011**, *62*, 1510–1520.
23. Kageyama, D.; Narita, S.; Watanabe, M. Insect sex determination manipulated by their endosymbionts: Incidences, mechanisms and implications. *Insects* **2012**, *3*, 161–199.

24. Subandiyah, S.; Nikoh, N.; Tsuyumu, S.; Somowiyarjo, S.; Fukatsu, T. Complex endosymbiotic microbiota of the citrus psyllid *Diaphorina citri* (Homoptera: Psylloidea). *Zool. Sci.* **2000**, *17*, 983–989.
25. Lemaitre, B.; Hoffmann, J. The host defense of *Drosophila melanogaster*. *Annu. Rev. Immunol.* **2007**, *25*, 697–743.
26. International Aphid Genomics Consortium Genome sequence of the pea aphid *Acyrtosiphon pisum*. *PLoS Biol.* **2010**, *8*, e1000313.
27. Baumann, P.; Moran, N.A.; Baumann, L.; Dworkin, M. Bacteriocyte-associated endosymbionts of insects. *Prokaryotes* **2006**, *1*, 403–438.
28. Buchner, P. *Endosymbiosis of Animals with Plant Microorganisms*; Interscience Publishers: New York, NY, USA, 1965.
29. Haine, E.R. Symbiont-mediated protection. *Proc. R. Soc. B Biol. Sci.* **2008**, *275*, 353–361.
30. Engelstädter, J.; Hurst, G.D. The ecology and evolution of microbes that manipulate host reproduction. *Annu. Rev. Ecol. Evol. Syst.* **2009**, *40*, 127–149.
31. Buchman, J.L.; Sengoda, V.G.; Munyaneza, J.E. Vector Transmission Efficiency of *Liberibacter* by *Bactericera cockerelli* (Hemiptera: Triozidae) in Zebra Chip Potato Disease: Effects of Psyllid Life Stage and Inoculation Access Period. *J. Econ. Entomol.* **2011**, *104*, 1486–1495.
32. Wallis, C.M.; Rashed, A.; Wallingford, A.K.; Rush, C.M. Relationship of potato biochemical responses to “*Candidatus Liberibacter solanacearum*”, causal agent of zebra chip, to disease progression. *Phytopathology* **2013**, *103*, 154–154.
33. Casteel, C.L.; Hansen, A.K.; Walling, L.L.; Paine, T.D. Manipulation of plant defense responses by the Tomato Psyllid (*Bactericera cockerelli*) and its associated endosymbiont *Candidatus Liberibacter Psyllauros*. *PLoS One* **2012**, *7*, e35191.
34. Grafton-Cardwell, E.E.; Stelinski, L.L.; Stansly, P.A. Biology and management of Asian citrus psyllid, vector of the Huanglongbing Pathogens. *Annu. Rev. Entomol.* **2013**, *58*, 413–432.
35. Munyaneza, J.E. Zebra chip disease of potato: Biology, epidemiology, and management. *Am. J. Potato Res.* **2012**, *89*, 329–350.
36. Wuriyangan, H.; Rosa, C.; Falk, B.W. Oral delivery of double-stranded RNAs and siRNAs induces RNAi effects in the potato/tomato psyllid, *Bactericera cockerelli*. *PLoS One* **2011**, *6*, e27736.
37. Wuriyangan, H.; Falk, B.W. RNA Interference towards the Potato Psyllid, *Bactericera cockerelli*, is induced in plants infected with recombinant *Tobacco mosaic virus* (TMV). *PLoS One* **2013**, *8*, e66050.
38. Lu, H.; Zhang, C.; Albrecht, U.; Shimizu, R.; Wang, G.; Bowman, K.D. Overexpression of a citrus NDR1 ortholog increases disease resistance in Arabidopsis. *Front. Plant Sci.* **2013**, *4*, doi:10.3389/fpls.2013.00157.
39. Soderlund, C.; Nelson, W.; Willer, M.; Gang, D.R. TCW: Transcriptome computational workbench. *PLoS One* **2013**, *8*, e69401.
40. Vyas, M.; Fisher, T.W.; Nelson, W.; Yin, G.; Cicero, J.M.; Willer, M.; Kim, R.; Kramer, R.; May, G.A.; Crow, J.A.; Soderlund, C.A.; Gang, D.R.; Brown, J.K. Stage-specific *Ca. Liberibacter*-infected Asian citrus psyllid expression profiles reveal exploitation nutrition and

- energy metabolism in adults and perturbed innate immunity and development in nymphs. *PLoS ONE*. **2014**, submitted.
41. Cicero, J.M.; Fisher, T.W.; Brown, J.K. are preparing the manuscript with title “Validation of the Candidatus *Liberibacter solanacearum*-morphotype by colloidal gold in situ hybridization and direct evidence of a flagellated form” 2014.
 42. Hung, T.H.; Hung, S.C.; Chen, C.N.; Hsu, M.H.; Su, H.J. Detection by PCR of *Candidatus Liberibacter asiaticus*, the bacterium causing citrus huanglongbing in vector psyllids: Application to the study of vector-pathogen relationships. *Plant Pathol.* **2004**, *53*, 96–102.
 43. Cicero, J.M.; Brown, J.K.; Roberts, P.D.; Stansly, P.A. The Digestive System of *Diaphorina citri* and *Bactericera cockerelli* (Hemiptera: Psyllidae). *Ann. Entomol. Soc. Am.* **2009**, *102*, 650–665.
 44. Robinson, M.D.; McCarthy, D.J.; Smyth, G.K. edgeR: A Bioconductor package for differential expression analysis of digital gene expression data. *Bioinformatics* **2010**, *26*, 139–140.
 45. Miller, J.R.; Koren, S.; Sutton, G. Assembly algorithms for next-generation sequencing data. *Genomics* **2010**, *95*, 315–327.
 46. Apweiler, R.; Martin, M.J.; O’Donovan, C.; Magrane, M.; Alam-Faruque, Y.; Antunes, R.; Barrell, D.; Bely, B.; Bingley, M.; Binns, D.; *et al.* UniProt Consortium The Universal Protein Resource (UniProt) in 2010. *Nucleic Acids Res.* **2010**, *38*, D142–D148.
 47. Apweiler, R.; Martin, M.J.; O’Donovan, C.; Magrane, M.; Alam-Faruque, Y.; Antunes, R.; Barrell, D.; Bely, B.; Bingley, M.; Binns, D.; *et al.* UniProt Consortium Ongoing and future developments at the Universal Protein Resource. *Nucleic Acids Res.* **2011**, *39*, D214–D219.
 48. Milius, S. Malaria mosquito dosed with disease-fighting bacteria, after thousands of tries lab gets parasite-carrying insect to catch Wolbachia. Available online: <https://www.sciencenews.org/article/malaria-mosquito-dosed-disease-fighting-bacteria> (accessed on 23 October 2014).
 49. Thao, M.L.; Moran, N.A.; Abbot, P.; Brennan, E.B.; Burckhardt, D.H.; Baumann, P. Cospeciation of psyllids and their primary prokaryotic endosymbionts. *Appl. Environ. Microbiol.* **2000**, *66*, 2898–2905.
 50. Lin, H.; Doddapaneni, H.; Chen, C.; Duan, Y.; Zhou, L.; Stenger, D.C.; Civerolo, E.L. Draft genome sequence of potato “Zebra Chip” associated bacterium “*Candidatus Liberibacter solanacearum*”. *Phytopathology* **2009**, *99*, S73–S73.
 51. Zou, H.; Gowda, S.; Zhou, L.; Hajeri, S.; Chen, G.; Duan, Y. The destructive citrus pathogen, “*Candidatus Liberibacter asiaticus*” encodes a functional flagellin characteristic of a pathogen-associated molecular pattern. *PLoS One* **2012**, e46447.
 52. Wairuri, C.K.; Van der Waals, Jacquie E; Van Schalkwyk, A.; Theron, J. *Ralstonia solanacearum* needs Flp pili for virulence on potato. *Mol. Plant-Microbe Interact.* **2012**, *25*, 546–556.
 53. Chiancone, E.; Ceci, P.; Ilari, A.; Ribacchi, F.; Stefanini, S. Iron and proteins for iron storage and detoxification. *BioMetals* **2004**, *17*, 197–202.
 54. Flipsen, J.; Mans, R.; Kleefman, A.; Knebel-Mürsdorf, D.; Vlak, J.M. Deletion of the baculovirus ecdysteroid UDP-glucosyltransferase gene induces early degeneration of Malpighian tubules in infected insects. *J. Virol.* **1995**, *69*, 4529–4532.
 55. Slack, J.M.; Kuzio, J.; Faulkner, P. Characterization of v-cath, a cathepsin L-like proteinase expressed by the baculovirus *Autographa californica* multiple nuclear polyhedrosis virus. *J. Gen. Virol.* **1995**, *76*, 1091–1098.

56. Cook, P.; McMeniman, C.; O'Neill, S. *Modifying Insect Population Age Structure to Control Vector-Borne Disease*; Aksoy, S., Ed.; Springer: New York, NY, USA, 2008; Volume 627, pp. 126–140.
57. Ashburner, M.; Ball, C.A.; Blake, J.A.; Botstein, D.; Butler, H.; Cherry, J.M.; Davis, A.P.; Dolinski, K.; Dwight, S.S.; Eppig, J.T.; *et al.* Gene Ontology Consortium Gene Ontology: Tool for the unification of biology. *Nat. Genet.* **2000**, *25*, 25–29.
58. Shen, Z.; Jacobs-Lorena, M. A Type I Peritrophic matrix protein from the Malaria vector *Anopheles gambiae* binds to chitin: Cloning, Expression, and Characterization. *J. Biol. Chem.* **1998**, *273*, 17665–17670.
59. Hegedus, D.; Erlandson, M.; Gillott, C.; Toprak, U. New insights into peritrophic matrix synthesis, architecture, and function. *Annu. Rev. Entomol.* **2009**, *54*, 285–302.
60. Schulte, R.D.; Makus, C.; Hasert, B.; Michiels, N.K.; Schulenburg, H. Multiple reciprocal adaptations and rapid genetic change upon experimental coevolution of an animal host and its microbial parasite. *Proc. Natl. Acad. Sci. USA* **2010**, *107*, 7359–7364.
61. Raddadi, N.; Gonella, E.; Camerota, C.; Pizzinat, A.; Tedeschi, R.; Crotti, E.; Mandrioli, M.; Bianco, P.A.; Daffonchio, D.; Alma, A. “*Candidatus Liberibacter europaeus*” sp. nov. that is associated with and transmitted by the psyllid *Cacopsylla pyri* apparently behaves as an endophyte rather than a pathogen. *Environ. Microbiol.* **2011**, *13*, 414–426.
62. Doucet, D.; Retnakaran, A. Insect Chitin: Metabolism, Genomics and Pest Management. *Insect Growth Disruptors* **2012**, *43*, 437–511.
63. Killiny, N.; Prado, S.S.; Almeida, R.P. Chitin utilization by the insect-transmitted bacterium *Xylella fastidiosa*. *Appl. Environ. Microbiol.* **2010**, *76*, 6134–6140.
64. Ortiz-Rodriguez, T.; de la Fuente-Salcido, N.; Bideshi, D.K.; Salcedo-Hernandez, R.; Barboza-Corona, J.E. Generation of chitin-derived oligosaccharides toxic to pathogenic bacteria using ChiA74, an endochitinase native to *Bacillus thuringiensis*. *Lett. Appl. Microbiol.* **2010**, *51*, 184–190.
65. Gerke, V.; Moss, S.E. Annexins and membrane dynamics. *Biochim. Biophys. Acta (BBA)-Mol. Cell Res.* **1997**, *1357*, 129–154.
66. Tjota, M.; Lee, S.K.; Wu, J.; Williams, J.A.; Khanna, M.R.; Thomas, G.H. Annexin B9 binds to beta(H)-spectrin and is required for multivesicular body function in *Drosophila*. *J. Cell. Sci.* **2011**, *124*, 2914–2926.
67. Kotsyfakis, M.; Ehret-Sabatier, L.; Siden-Kiamos, I.; Mendoza, J.; Sinden, R.E.; Louis, C. Plasmodium berghei ookinetes bind to *Anopheles gambiae* and *Drosophila melanogaster* annexins. *Mol. Microbiol.* **2005**, *57*, 171–179.
68. Lavine, M.; Strand, M. Insect hemocytes and their role in immunity. *Insect Biochem. Mol. Biol.* **2002**, *32*, 1295–1309.
69. Ratzka, C.; Gross, R.; Feldhaar, H. Endosymbiont Tolerance and Control within Insect Hosts. *Insects* **2012**, *3*, 553–572.
70. Wang, N.; Trivedi, P. Citrus huanglongbing: A newly relevant disease presents unprecedented challenges. *Phytopathology* **2013**, *103*, 652–665.
71. Kovács, Á.T.; van Gestel, J.; Kuipers, O.P. The protective layer of biofilm: A repellent function for a new class of amphiphilic proteins. *Mol. Microbiol.* **2012**, *85*, 8–11.

72. Bastian, F.O.; Elzer, P.H.; Wu, X. *Spiroplasma* spp. biofilm formation is instrumental for their role in the pathogenesis of plant, insect and animal diseases. *Exp. Mol. Pathol.* **2012**, *93*, 116–128.
73. Nachappa, P.; Levy, J.; Tamborindeguy, C. Transcriptome analyses of *Bactericera cockerelli* adults in response to “*Candidatus Liberibacter solanacearum*” infection. *Mol. Genet. Genomics* **2012**, *287*, 803–817.
74. Leulier, F.; Rodriguez, A.; Khush, R.S.; Abrams, J.M.; Lemaitre, B. The *Drosophila* caspase Dredd is required to resist gram-negative bacterial infection. *EMBO Rep.* **2000**, *1*, 353–358.
75. Doyle, S.E.; O’Connell, R.M.; Miranda, G.A.; Vaidya, S.A.; Chow, E.K.; Liu, P.T.; Suzuki, S.; Suzuki, N.; Modlin, R.L.; Yeh, W. Toll-like receptors induce a phagocytic gene program through p38. *J. Exp. Med.* **2004**, *199*, 81–90.
76. Valanne, S.; Wang, J.; Rännet, M. The *Drosophila* Toll Signaling Pathway. *J. Immunol.* **2011**, *186*, 649–656.
77. Flannagan, R.S.; Jaumouillé V.; Grinstein, S. The cell biology of phagocytosis. *Annu. Rev. Pathol. Mech. Dis.* **2012**, *7*, 61–98.
78. Mansueto, P.; Vitale, G.; Cascio, A.; Seidita, A.; Pepe, I.; Carroccio, A.; di Rosa, S.; Rini, G.B.; Cillari, E.; Walker, D.H. New insight into immunity and immunopathology of Rickettsial diseases. *Clin. Dev. Immunol.* **2012**, 2–26.
79. Cossart, P.; Veiga, E. Non-classical use of clathrin during bacterial infections. *J. Microsc.* **2008**, *231*, 524–528.
80. Sarantis, H.; Grinstein, S. Subversion of phagocytosis for pathogen survival. *Cell Host Microbe* **2012**, *12*, 419–431.
81. Hudson, B.I.; Kalea, A.Z.; del Mar Arriero, M.; Harja, E.; Boulanger, E.; D’Agati, V.; Schmidt, A.M. Interaction of the RAGE cytoplasmic domain with diaphanous-1 is required for ligand-stimulated cellular migration through activation of Rac1 and Cdc42. *J. Biol. Chem.* **2008**, *283*, 34457–34468.
82. Castellano, F.; Montcourrier, P.; Chavrier, P. Membrane recruitment of Rac1 triggers phagocytosis. *J. Cell. Sci.* **2000**, *113*, 2955–2961.
83. Fu, Y.; Galán, J.E. A *Salmonella* protein antagonizes Rac-1 and Cdc42 to mediate host-cell recovery after bacterial invasion. *Nature* **1999**, *401*, 293–297.
84. Kontani, K.; Tada, M.; Ogawa, T.; Okai, T.; Saito, K.; Araki, Y.; Katada, T. Di-Ras, a distinct subgroup of ras family GTPases with unique biochemical properties. *J. Biol. Chem.* **2002**, *277*, 41070–41078.
85. Kim, J.; Moon, M.; Kim, H.; Li, Y.; Song, D.; Kim, J.; Lee, J.; Kim, J.; Kim, S.; Park, J. Ras-related GTPases Rap1 and RhoA collectively induce the phagocytosis of serum-opsonized zymosan particles in macrophages. *J. Biol. Chem.* **2012**, *287*, 5145–5155.
86. Akbar, M.A.; Tracy, C.; Kahr, W.H.; Krämer, H. The full-of-bacteria gene is required for phagosome maturation during immune defense in *Drosophila*. *J. Cell Biol.* **2011**, *192*, 383–390.
87. Parker, H.; Chitcholtan, K.; Hampton, M.B.; Keenan, J.I. Uptake of *Helicobacter pylori* outer membrane vesicles by gastric epithelial cells. *Infect. Immun.* **2010**, *78*, 5054–5061.
88. Jin, T.; Satoh, T.; Liao, Y.; Song, C.; Gao, X.; Kariya, K.; Hu, C.; Kataoka, T. Role of the CDC25 homology domain of phospholipase Cε in amplification of Rap1-dependent signaling. *J. Biol. Chem.* **2001**, *276*, 30301–30307.

89. Lopez, I.; Mak, E.C.; Ding, J.; Hamm, H.E.; Lomasney, J.W. A novel bifunctional phospholipase C that is regulated by Gα12 and stimulates the Ras/mitogen-activated protein kinase pathway. *J. Biol. Chem.* **2001**, *276*, 2758–2765.
90. Lin, H.; Lou, B.; Glynn, J.M.; Doddapaneni, H.; Civerolo, E.L.; Chen, C.; Duan, Y.; Zhou, L.; Vahling, C.M. The complete genome sequence of “*Candidatus Liberibacter solanacearum*”, the bacterium associated with potato zebra chip disease. *PLoS One* **2011**, *6*, e19135.
91. Battaile, K.P.; McBurney, M.; Van Veldhoven, P.P.; Vockley, J. Human long chain, very long chain and medium chain acyl-CoA dehydrogenases are specific for the S-enantiomer of 2-methylpentadecanoyl-CoA. *Biochim. Biophys. Acta-Lipids Lipid Metab.* **1998**, *1390*, 333–338.
92. Kazakov, A.E.; Rodionov, D.A.; Alm, E.; Arkin, A.P.; Dubchak, I.; Gelfand, M.S. Comparative Genomics of Regulation of Fatty Acid and Branched-Chain Amino Acid Utilization in Proteobacteria. *J. Bacteriol.* **2009**, *191*, 52–64.
93. Falabella, P.; Riviello, L.; Stradis, M.D.; Stigliano, C.; Varricchio, P.; Grimaldi, A.; Eguileor, M.D.; Graziani, F.; Gigliotti, S.; Pennacchio, F. *Aphidius ervi* teratocytes release an extracellular enolase. *Insect Biochem. Mol. Biol.* **2009**, *39*, 801–813.
94. Mitra, S.; Cui, J.; Robbins, P.W.; Samuelson, J. A deeply divergent phosphoglucomutase (PGM) of *Giardia lamblia* has both PGM and phosphomannomutase activities. *Glycobiology* **2010**, *20*, 1233–1240.
95. Lazarevic, V.; Soldo, B.; Médico, N.; Pooley, H.; Bron, S.; Karamata, D. *Bacillus subtilis* α-Phosphoglucomutase Is Required for Normal Cell Morphology and Biofilm Formation. *Appl. Environ. Microbiol.* **2005**, *71*, 39–45.
96. Runyen-Janecky, L.J.; Brown, A.N.; Ott, B.; Tujuba, H.G.; Rio, R.V. Regulation of high-affinity iron acquisition homologues in the tsetse fly symbiont *Sodalis glossinidius*. *J. Bacteriol.* **2010**, *192*, 3780–3787.
97. Meyron-Holtz, E.G.; Moshe-Belizowski, S.; Cohen, L.A. A possible role for secreted ferritin in tissue iron distribution. *J. Neural Transm.* **2011**, *118*, 337–347.
98. Tran, S.L.; Guillemet, E.; Lereclus, D.; Ramarao, N. Iron regulates *Bacillus thuringiensis* haemolysin hlyII gene expression during insect infection. *J. Invertebr. Pathol.* **2013**, *113*, 205–208.
99. Arosio, P.; Ingrassia, R.; Cavadini, P. Ferritins: A family of molecules for iron storage, antioxidation and more. *Biochim. Biophys. Acta (BBA)-Gen. Subj.* **2009**, *1790*, 589–599.
100. Kim, B.Y.; Lee, K.S.; Choo, Y.M.; Kim, I.; Je, Y.H.; Woo, S.D.; Lee, S.M.; Park, H.C.; Sohn, H.D.; Jin, B.R. Insect transferrin functions as an antioxidant protein in a beetle larva. *Comp. Biochem. Physiol. Part B Biochem. Mol. Biol.* **2008**, *150*, 161–169.
101. Gabaldon, T.; Koonin, E.V. Functional and evolutionary implications of gene orthology. *Nat. Rev. Genet.* **2013**, *14*, 360–366.
102. Iseli, C.; Jongeneel, C.V.; Bucher, P. ESTScan: A program for detecting, evaluating, and reconstructing potential coding regions in EST sequences. *Proc. Int. Conf. Intell. Syst. Mol. Biol.* **1999**, 138–148.
103. Li, L.; Stoeckert, C.J., Jr.; Roos, D.S. OrthoMCL: Identification of ortholog groups for eukaryotic genomes. *Genome Res.* **2003**, *13*, 2178–2189.
104. Lee Rodgers, J.; Nicewander, W.A. Thirteen ways to look at the correlation coefficient. *Am. Stat.* **1988**, *42*, 59–66.

105. Goh, K.; Cusick, M.E.; Valle, D.; Childs, B.; Vidal, M.; Barabasi, A. The human disease network. *Proc. Natl. Acad. Sci. USA* **2007**, *104*, 8685–8690.
106. Aruni, W.; Vanterpool, E.; Osbourne, D.; Roy, F.; Muthiah, A.; Dou, Y.; Fletcher, H.M. Sialidase and Sialoglycoproteases Can Modulate Virulence in *Porphyromonas gingivalis*. *Infect. Immun.* **2011**, *79*, 2779–2791.
107. Severi, E.; Hood, D.W.; Thomas, G.H. Sialic acid utilization by bacterial pathogens. *Microbiology* **2007**, *153*, 2817–2822.
108. Wallace, A.J.; Stillman, T.J.; Atkins, A.; Jamieson, S.J.; Bullough, P.A.; Green, J.; Artymiuk, P.J. E. coli hemolysin E (HlyE, ClyA, SheA): X-ray crystal structure of the toxin and observation of membrane pores by electron microscopy. *Cell* **2000**, *100*, 265–276.
109. Zitzer, A.; Zitzer, O.; Bhakdi, S.; Palmer, M. Oligomerization of *Vibrio cholerae* cytolysin yields a pentameric pore and has a dual specificity for cholesterol and sphingolipids in the target membrane. *J. Biol. Chem.* **1999**, *274*, 1375–1380.
110. Amino, R.; Martins, R.M.; Procopio, J.; Hirata, I.Y.; Juliano, M.A.; Schenkman, S. Trialysin, a novel pore-forming protein from saliva of hematophagous insects activated by limited proteolysis. *J. Biol. Chem.* **2002**, *277*, 6207–6213.
111. Petersen, U.; Kadalayil, L.; Rehorn, K.; Hoshizaki, D.K.; Reuter, R.; Engström, Y. Serpent regulates *Drosophila* immunity genes in the larval fat body through an essential GATA motif. *EMBO J.* **1999**, *18*, 4013–4022.
112. Ennes-Vidal, V.; Menna-Barreto, R.F. S.; Santos, A.L. S.; Branquinha, M.H.; d'Avila-Levy, C.M. MDL28170, a Calpain Inhibitor, Affects *Trypanosoma cruzi* metacyclogenesis, ultrastructure and attachment to *Rhodnius prolixus* midgut. *PLoS One* **2011**, *6*, e18371.
113. Patt, J.; S éamou, M. Responses of the Asian citrus psyllid to volatiles emitted by the flushing shoots of its rutaceous host plants. *Environ. Entomol.* **2010**, *39*, 618–624.
114. Xu, K.; Broder, C.C.; Nikolov, D.B. Ephrin-B2 and Ephrin-B3 as Functional Henipavirus Receptors. *Semin. Cell Dev. Biol.* **2012**, *23*, 116–123.
115. Nilius, B.; Owsianik, G. The transient receptor potential family of ion channels. *Genome Biol.* **2011**, doi:10.1186/gb-2011-12-3-218.
116. Schroder, H.C.; Ushijima, H.; Krasko, A.; Gamulin, V.; Thakur, N.L.; Diehl-Seifert, B.; Muller, I.M.; Muller, W.E. Emergence and disappearance of an immune molecule, an antimicrobial lectin, in basal metazoa. A tachylectin-related protein in the sponge *Suberites domuncula*. *J. Biol. Chem.* **2003**, *278*, 32810–32817.
117. Reiko, F.; Shusaku, I.; Yoshimitsu, K.; Toshitsugu, U.; Yoshiko, M. Characterization of tectonins I and II from *Physarum polycephalum*. *Adv. Biol. Chem.* **2012**, doi:10.4236/abc.2012.23032.
118. Heung, L.J.; Luberto, C.; del Poeta, M. Role of sphingolipids in microbial pathogenesis. *Infect. Immun.* **2006**, *74*, 28–39.
119. Rajakumari, S.; Rajasekharan, R.; Daum, G. Triacylglycerol lipolysis is linked to sphingolipid and phospholipid metabolism of the yeast *Saccharomyces cerevisiae*. *Biochim. Biophys. Acta (BBA)-Mol. Cell Biol. Lipids* **2010**, *1801*, 1314–1322.
120. Lattif, A.A.; Mukherjee, P.K.; Chandra, J.; Roth, M.R.; Welti, R.; Rouabhia, M.; Ghannoum, M.A. Lipidomics of *Candida albicans* biofilms reveals phase-dependent production of phospholipid molecular classes and role for lipid rafts in biofilm formation. *Microbiology* **2011**, *157*, 3232–3242.

121. Swisher, K.D.; Munyaneza, J.E.; Crosslin, J.M. High resolution melting analysis of the cytochrome oxidase I gene identifies three haplotypes of the potato psyllid in the United States. *Environ. Entomol.* **2012**, *41*, 1019–1028.
122. Jagoueix, S.; Bové J.M.; Garnier, M. PCR detection of the two *Candidatus liberobacter* species associated with greening disease of citrus. *Mol. Cell. Probes* **1996**, *10*, 43–50.
123. He, R.; Kim, M.J.; Nelson, W.; Balbuena, T.S.; Kim, R.; Kramer, R.; Crow, J.A.; May, G.D.; Thelen, J.J.; Soderlund, C.A.; *et al.* Next-generation sequencing-based transcriptomic and proteomic analysis of the common reed, *Phragmites australis* (Poaceae), reveals genes involved in invasiveness and rhizome specificity. *Am. J. Bot.* **2012**, *99*, 232–247.
124. Birol, I.; Jackman, S.D.; Nielsen, C.B.; Qian, J.Q.; Varhol, R.; Stazyk, G.; Morin, R.D.; Zhao, Y.; Hirst, M.; Schein, J.E.; *et al.* De novo transcriptome assembly with ABySS. *Bioinformatics* **2009**, *25*, 2872–2877.
125. Li, R.; Yu, C.; Li, Y.; Lam, T.; Yiu, S.; Kristiansen, K.; Wang, J. SOAP2: An improved ultrafast tool for short read alignment. *Bioinformatics* **2009**, *25*, 1966–1967.
126. Chevreux, B.; Pfisterer, T.; Drescher, B.; Driesel, A.J.; Muller, W.E. G.; Wetter, T.; Suhai, S. Using the miraEST assembler for reliable and automated mRNA transcript assembly and SNP detection in sequenced ESTs. *Genome Res.* **2004**, *14*, 1147–1159.
127. Li, W.; Godzik, A. Cd-hit: A fast program for clustering and comparing large sets of protein or nucleotide sequences. *Bioinformatics* **2006**, *22*, 1658–1659.
128. Li, H.; Durbin, R. Fast and accurate short read alignment with Burrows-Wheeler transform. *Bioinformatics* **2009**, *25*, 1754–1760.
129. Young, M.; Wakefield, M.; Smyth, G.; Oshlack, A. Gene ontology analysis for RNA-seq: Accounting for selection bias. *Genome Biol.* **2010**, doi:10.1186/gb-2010-11-2-r14.

© 2014 by the authors; licensee MDPI, Basel, Switzerland. This article is an open access article distributed under the terms and conditions of the Creative Commons Attribution license (<http://creativecommons.org/licenses/by/4.0/>).